Structure-Based Discovery and Optimization of Benzo[*d*]isoxazole Derivatives as Potent and Selective BET Inhibitors for Potential Treatment of Castration-Resistant Prostate Cancer (CRPC)

Maofeng Zhang, Yan Zhang, Ming Song, Xiaoqian Xue, Junjian Wang, Chao Wang, Cheng Zhang, Chenchang Li, Qiuping Xiang, Lingjiao Zou, Xishan Wu, Chun Wu, Baijun Dong, Wei Xue, Yulai Zhou, Hongwu Chen, Donghai Wu, Ke Ding, and Yong Xu

J. Med. Chem., **Just Accepted Manuscript** • DOI: 10.1021/acs.jmedchem.8b00103 • Publication Date (Web): 22 Mar 2018

Structure-Based Discovery and Optimization of Benzo[*d*]isoxazole Derivatives as Potent and Selective BET Inhibitors for Potential Treatment of Castration-Resistant Prostate Cancer (CRPC)

Maofeng Zhang,[†,‡,#] Yan Zhang,[†,‡,#] Ming Song,[†,#] Xiaoqian Xue,[†,‡] Junjian Wang,[¶] Chao Wang,[†] Cheng Zhang,[†,§] Chenchang Li,[†,§] Qiuping Xiang,[†,‡] Lingjiao Zou,[†,‡] Xishan Wu,[†,‡] Chun Wu,[†] Baijun Dong,[∥] Wei Xue,[∥] Yulai Zhou,[§] Hongwu Chen,[¶] Donghai Wu,[†] Ke Ding,[▽] and Yong Xu[†,*]

[†]Guangdong Provincial Key Laboratory of Biocomputing, Joint School of Life Sciences, Guangzhou Institutes of Biomedicine and Health, Chinese Academy of Sciences, Guangzhou 510530; Guangzhou Medical University, Guangzhou 511436, China.

[‡]University of Chinese Academy of Sciences, No. 19 Yuquan Road, Beijing 100049, China.

[§]School of Pharmaceutical Sciences, Jilin University, No. 1266 Fujin Road, Chaoyang District, Changchun, Jilin 130021, China.

[¶]Department of Biochemistry and Molecular Medicine, School of Medicine, University of California, Davis, Sacramento, California 95817, USA.

[∥]Department of Urology, Renji Hospital, School of Medicine, Shanghai Jiao Tong University, Shanghai 200127, China.

[▽]School of Pharmacy, Jinan University, 601 Huangpu Avenue West, Guangzhou 510632, China.

[*]Corresponding Author: Yong Xu, PhD, E-mail: xu_yong@gibh.ac.cn

[#]These authors contributed equally to this work.

KEYWORDS: BRD, Bromodomain, Benzo[*d*]isoxazole, Prostate Cancer, CRPC

ABSTRACT

The bromodomain and extra-terminal (BET) family proteins have gained increasing interest as drug targets for treatment of castration-resistant prostate cancer (CRPC). Here, we describe the design, optimization and evaluation of benzo[*d*]isoxazole-containing compounds as potent BET bromodomain inhibitors. Co-crystal structures of the representative inhibitors in complex with BRD4(1) provided solid structural basis for compound optimization. The two most potent compounds, **6i** (Y06036) and **7m** (Y06137), bound to the BRD4(1) bromodomain with K_d values of 82 and 81 nM, respectively. They also exhibited high selectivity over other non-BET subfamily members. The compounds potently inhibited cell growth, colony formation, and the expression of AR, AR regulated genes, and MYC in prostate cancer cell lines. Compounds **6i** and **7m** also demonstrated therapeutic effects in a C4-2B CRPC xenograft tumor model in mice. These potent and selective BET inhibitors represent a new class of compounds for the development of potential therapeutics against CRPC.

1. INTRODUCTION

Prostate cancer (PCa) is the most common malignancy and the fifth leading cause of death from malignancy in men.[1-3] Since androgen receptor (AR) signaling has a pivotal role in PCa, androgen deprivation therapy (ADT) with surgical or chemical castration is the standard treatment with most patients going to remission.[4-6] However, the disease progresses to an incurable stage known as castration-resistant prostate cancer (CRPC). Most patients initially benefit from and eventually develop resistance to second-generation therapies such as enzalutamide (Enz) and abiraterone (Abi).[7-9] Therefore, the development of new strategies to tackle AR signaling in CRPC is urgently needed.

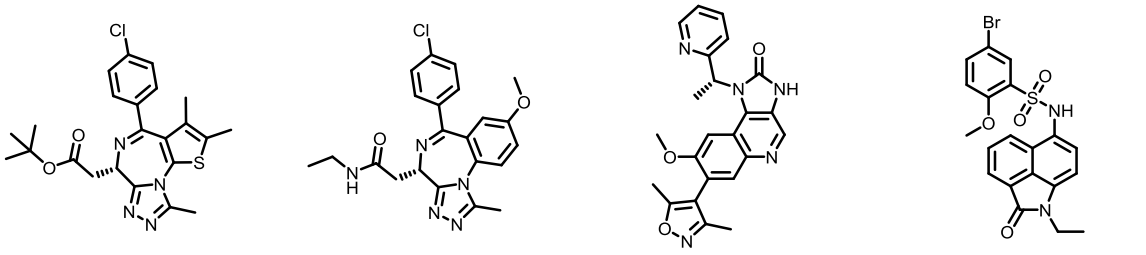

Figure 1. Structures of representative BET bromodomain inhibitors including (+)-JQ1 (**1**), I-BET762 (**2**), I-BET151 (**3**), and Y02224 (**4**). The IC_{50} values were obtained using different methods and are given in italics.

Bromodomain and extra terminal domain (BET) family proteins, including BRD2, BRD3, BRD4, and BRDT, bind to acetylated lysines via their tandem domains (BD1 and BD2) to regulate gene transcription. These proteins have emerged as new therapeutic targets for human diseases and conditions, including cancers[10-15] and inflammation.[16,17] There has been significant progress in

the development of small molecule inhibitors targeting the BET bromodomains. These potent and selective inhibitors, such as (+)-JQ1 (**1**),[18] I-BET762 (**2**),[19-21] and I-BET151 (**3**)[10,22] (Figure 1), can significantly inhibit tumor growth in xenograft models in mice. We previously reported the design of a new class of BET bromodomain inhibitors containing a benzo[*cd*]indol-2(1*H*)-one structure, exemplified by Y02224 (**4**, Figure 1), which exhibited reasonable antiproliferative effect on leukemia cells.[23]

Chinnaiyan and others have shown that BRD4 inhibitors can disrupt the AR–BD1 interactions, induce down-regulation of AR-regulated genes, and inhibit tumor growth in CRPC xenograft mouse models.[12,13,19] BET family proteins have been gaining increasing interest as drug targets for treatment of CRPC.[24-26] Therefore, targeting BET proteins represents an alternative strategy for treatment of CRPC. Despite the discovery of these BET inhibitors, chemicals that entered clinical trials for CRPC are still limited. BET inhibitors **2**, OTX-015, ZEN003694 and GS-5829, are currently being evaluated in clinical trials in patients with CRPC as a single agent or in combination with AR-antagonists (Enz or ARN-509).[27-30] Thus, potent and selective BET inhibitors with different chemotypes are still in high demand to enhance our understanding of the therapeutic potential of BET inhibition.

In the present study, we report the structure-based design, synthesis, and biological evaluation of a new class of potent and specific small molecular BET inhibitors, the benzo[*d*]isoxazoles, for potential treatment of CRPC.

2. RESULTS AND DISCUSSION

2.1. Design and Optimization of Benzo[*d*]isoxazole Derivatives.

2.1.1. Design of Benzo[*d*]isoxazole Scaffold.

To identify a novel scaffold, all available co-crystal structures of BET proteins and their inhibitors were aligned to explore the key pharmacophore elements. From the structural analysis, it is obvious that the ligands may form direct or indirect hydrogen bonds with Asn140 and Tyr97 and hydrophobic interactions with the WPF shelf. Some additional interactions near the BC and ZA channels may also contribute to ligand binding. In this study, the representative BET inhibitors **1**, **2** and **3** were used to produce a new scaffold (3-methylbenzo[*d*]isoxazole) through a hybridization approach (Figure 2). From the predicted binding mode analysis by molecular docking, we can see that the 3-methylbenzo[*d*]isoxazole moiety fits snugly into the KAc binding pocket and forms hydrogen bonds to a conserved water molecule and residue Asn140 (Figure 2). Starting from this scaffold, various substituents, such as sulfonamide derivatives as disclosed in our previous patent[31] and conformation restrained benzimidazole derivatives as disclosed in patents from Boehringer Ingelheim[32-34] and GlaxoSmithKline[35], were designed to explore the chemical space for potency improvement.

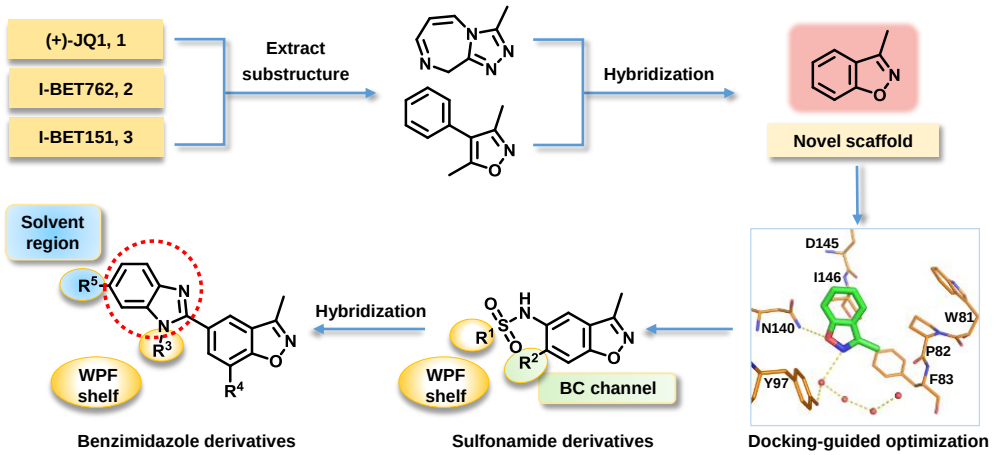

Figure 2. Flowchart summarizing the discovery and optimization strategy for novel benzo[*d*]isoxazole-containing BET inhibitors. Crystal structure of BRD4(1) with inhibitor **1** (PDB ID: 3MXF) were used for model construction.

2.1.2. SAR Studies of Sulfonamide Derivatives Occupying the WPF shelf.

To find potent benzo[*d*]isoxazole derivatives, we designed various substituents pointing to the WPF shelf region with a sulfonamide linker to explore the chemical space (Figure 2). First, lipophilic alkyl or cycloalkyl substituted compounds **5a–5e** were synthesized (Table 1). Utilizing the thermal shift assay (TSA) and the AlphaScreen assay, the compounds were evaluated for their abilities to bind to the BRD4(1) bromodomain. The well characterized inhibitor **1** was included as a reference compound to validate all the experimental procedures. Fortunately, these compounds exhibited moderate potencies. Among them, compound **5e** with a cyclohexyl group at R^1 position displayed a thermal shift of 4.5 ℃ and an IC_{50} value of 2.24 μM. Aromatic derivatives were also synthesized to investigate the SAR. As shown in Table 1, the phenyl derivative **5f** exhibited a weaker potency compared to the corresponding aliphatic compound **5e**. However, regardless of the substitution of an electron withdrawing group -Cl (**5h**), $-NO_2$ (**5i**), or electron-donating group $-OCH_3$ (**5j**), substitutions at para-position of phenyl ring were detrimental to BRD4(1) binding. The results suggested there was no chemical space at the para-position of phenyl ring for affinity improvement. In contrast, compounds with phenyl ring ortho-substitutions displayed encouraging results. For example, compound **5k** exhibited a thermal shift of 5.2 °C and an IC_{50} value of 1.59 μM. When the 2-chloro group at the ortho-position in **5k** was replaced with -Br, $-COOCH_3$ or –COOH (**5l–5n**), the compounds showed slightly decreased potencies.

Table 1. Structure−Activity Relationships of Compounds **5a−5v** for BRD4 (1) Activities[a]

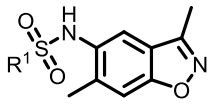

No.	R^1	TSA ΔT_m (°C)	AlphaScreen (μM)
1	-	11.5	0.12 ± 0.01
5a		3.0	5.30 ± 0.63
5b		4.5	2.47 ± 0.13
5c		5.0	2.55 ± 0.01
5d		5.0	3.05 ± 0.54
5e		4.5	2.24 ± 0.27
5f		2.0	4.96 ± 1.18
5g	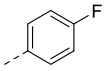	2.0	9.82 ± 0.84
5h	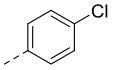	1.0	>20
5i	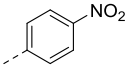	0.5	>20
5j	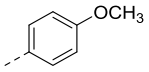	1.5	>20
5k		5.2	1.59 ± 0.17
5l		4.4	1.84 ± 0.11
5m	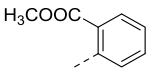	3.0	6.93 ± 2.01
5n	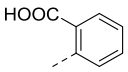	3.8	5.81 ± 1.34

5o	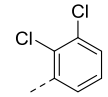	4.0	3.55 ± 0.49
5p	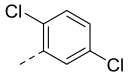	5.0	2.35 ± 0.92
5q	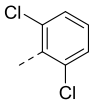	1.1	>20
5r	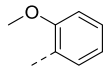	6.6	0.83 ± 0.01
5s	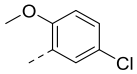	6.5	1.05 ± 0.43
5t	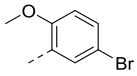	7.5	0.62 ± 0.09
5u	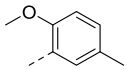	4.6	2.13 ± 1.06
5v	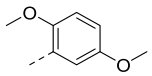	2.0	10.68 ± 3.18

[a]The IC_{50} of all compounds in the table were calculated from at least two independent experiments. Values are given as the mean ± SD.

Considering the good potency of compound **5k**, we kept the ortho chlorine and further added various substituents at other positions in the phenyl ring. Thus, **5o–5q** were designed and synthesized. Among them, the 2,5-disubstituted compound (**5p**) showed a similar potency compared to **5k**. To better design potent compounds, we predicted the binding mode of **5p** with BRD4(1) using a molecular docking approach. When the structures of compound **5p** and compound **4** in complex with BRD4(1) were superimposed (Supporting Information, Figure S1A), the phenyl groups overlapped very well. The 2-methoxy on the phenyl motif of **4** was found to form a hydrogen bond with the 7th solvent water. This discovery encouraged us to design 2-methoxy compounds. As expected, the 2-methoxy compound **5r** displayed an increased potency with a thermal shift of 6.6 ℃ and an IC_{50} value of 0.83 μM. When a chloro group was

introduced at 5-position, the resulting compound (**5s**) achieved no improvement in potency. Replacement of the 5-chloro (**5s**) with 5-bromo (**5t**) led to an increased activity, with a thermal shift of 7.5 ℃ and an IC_{50} value of 0.62 μM. The size of the substituent at the 5-position may be important for compound activity. When the 5-bromo group was replaced with a methoxy group (**5v**), the compound activity decreased approximately 20-fold as evaluated by the AlphaScreen assay.

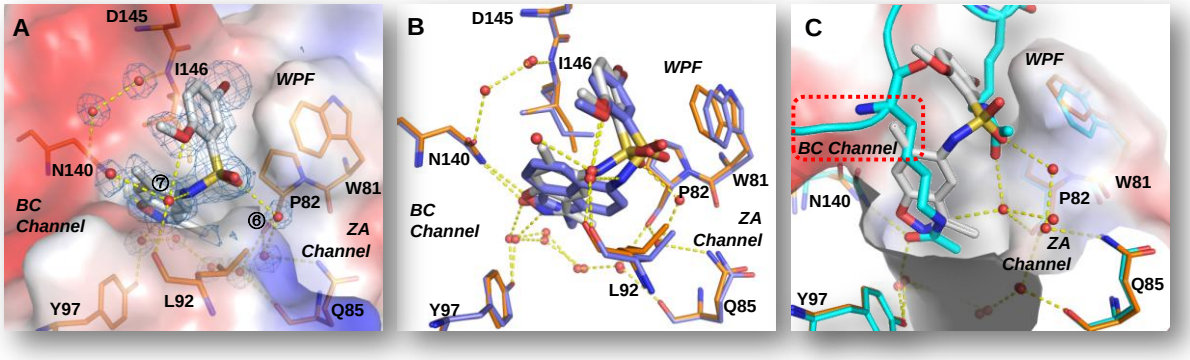

Figure 3. (A) X-ray crystal structure of **5t** in complex with BRD4(1) (PBD ID: 5Y8Z, carbon: gray); the electronic density of the ligand and water molecules are shown in the contour map. (B) Overlaid X-ray crystal structures of **5t** (PBD ID: 5Y8Z, carbon: gray) and compound **4** (PBD ID: 5DX4, carbon: violet) in complex with BRD4(1). (C) Overlaid X-ray crystal structures of **5t** (PBD ID: 5Y8Z, carbon: gray) and diacetylated histone peptide (PBD ID: 3UVW, carbon: cyan) in complex with BRD4(1).

To understand the structural basis for the high binding affinity of compound **5t** to the BRD4(1) protein, we determined the co-crystal structure of **5t** in complex with BRD4(1) at 1.84 Å resolution (Figure 3A). The overall binding mode was consistent with our initial docking

prediction. The 3-methylbenzo[*d*]isoxazole motif resided deep in the KAc-binding pocket with the oxygen atom forming a hydrogen bond with Asn140. The isoxazole ring nitrogen atom formed a water-mediated hydrogen bond with Tyr97. The 3-methyl group fitted well into the cavity formed by the remaining water molecules and occupied the sub-pocket that accommodated the acetyl group of acetylated lysine. The sulfonamide linker formed a vector that enabled the attached R^1-motif to occupy the WPF shelf. One of the sulfonamide linker oxygen atoms formed a hydrogen bond interaction with the 6th water located in the ZA channel. This solvent water presented a suitable geometry to enable the water-mediated hydrogen bond network with the bottom conserved water molecules. As expected, the 2-methoxy and NH formed hydrogen bonds with the 7th water molecule, which was consistent with that of compound **4** (Figure 3B). This water molecule also formed additional hydrogen bond interactions with the carbonyl group of Leu92 and another solvent water molecule.

2.1.3. SAR Studies of Sulfonamide Derivatives towards the BC Channel.

The next region for SAR study was the BC channel. Previous studies by Filippakopoulos reported the co-crystal structure of a diacetylated histone peptide bound to BRD4(1).[36] The peptide extended from the WPF shelf to the BC channel region. When the X-ray crystal structure of **5t**–BRD4(1) was overlaid with the co-crystal structure of the diacetylated histone peptide H4K5$_{Ac}$K8$_{Ac}$–BRD4(1) (PDB ID: 3UVW, Figure 3C),[36] the 6-methyl group of benzo[*d*]isoxazole scaffold pointed to the main chain of the histone H4 acetylated lysine mark (K5$_{Ac}$). Inspired by this, we designed some peptide mimics to occupy the peptide binding groove (BC channel). Due to the hydrophilic and high electrostatic potential properties of the BC channel, compounds **6a–6f** were synthesized with amide linkages and polar substituents (Table

2). However, the compounds with longer and hydrophilic substituents showed moderate inhibitory activities. It was obvious that shorter substitution at the R^2 position (**6a**) exhibited higher affinity (ΔT_m = 9.2 ℃; IC_{50} = 0.23 μM). To understand the structural basis for further structure-guided optimizations, compounds **6e** and **6f** were co-crystallized with BRD4(1). Due to the flexibility of the substituent in **6e**, the electron-density analysis indicated that a long substituent at the R^2 position exhibited an unstable conformation. The amide in **6f** formed a hydrogen bond with the 7th solvent water, which further bound to Leu92. The morpholine ring at the end of the chain extended to the top of BC channel and showed fewer key interactions with the protein (Supporting Information, Figure S1B).

Table 2. Structure−Activity Relationships of Compounds **6a**, **6c−6n** for BRD4(1) Activities[a]

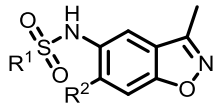

No.	R^1	R^2	TSA ΔT_m (°C)	AlphaScreen (μM)
6a	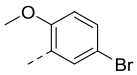	-OH	9.2	0.23 ± 0.01
6c	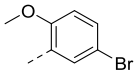	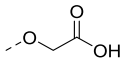	6.2	0.58 ± 0.03
6d	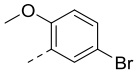	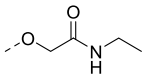	5.1	1.60 ± 0.23
6e	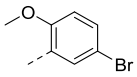	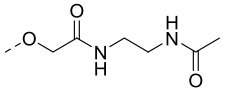	5.4	0.75 ± 0.01
6f	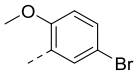	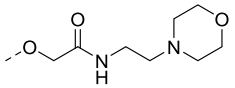	4.8	2.27 ± 1.24
6g	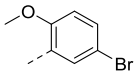		6.0	0.42 ± 0.01

6h	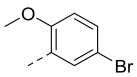	-OCH_2CH_3	9.2	0.15 ± 0.05
6i	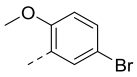	-OCH_3	9.8	0.13 ± 0.01
6j	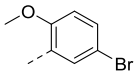	-$NHCH_3$	9.2	0.15 ± 0.04
6k		-OCH_3	7.8	0.22 ± 0.00
6l	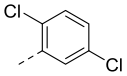	-OCH_3	7.3	0.44 ± 0.03
6m	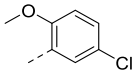	-OCH_3	8.7	0.16 ± 0.04
6n	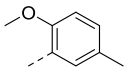	-OCH_3	7.8	0.47 ± 0.03

[a]The IC_{50} of all compounds in the table were calculated from at least two independent experiments. Values are given as the mean ± SD.

Based on the above analysis, we decided to focus on smaller R^2 substituents, leading to the synthesis of compounds **6g**, **6h** and **6i**. The results demonstrated that the 6-methoxy group (**6i**) was optimal for BRD4(1) binding potency. **6i** was almost identical to that of reference compound **1** with an IC_{50} value of 0.13 μM. When a little larger group, such as propoxy group (**6g**), was introduced at the R^2 position, the compound potency decreased approximately 3-fold. Thus far, the structure-activity relationships have established that the R^2-position favors small groups.

To understand the structural basis for the SAR, we determined the co-crystal structures of **6a**, **6i**, and **6j** bound to BRD4(1). As shown in Figures 4A and 4B, 6-OH derivative **6a** and 6-OCH_3 derivative **6i** formed hydrogen bond interactions with the 7th solvent water molecule.

Importantly, the 6-OCH_3 in **6i** occupied the position of the acetylated lysine ($K5_{Ac}$) hydrophobic chain. Similarly, the 6-$NHCH_3$ derivative **6j** displayed similar binding affinity to the 6-OCH_3 derivative **6i**. The crystal structure of **6j** bound to BRD4(1) indicated that the solvent water-mediated hydrogen bonds were important for the high potency (Figure 4C).

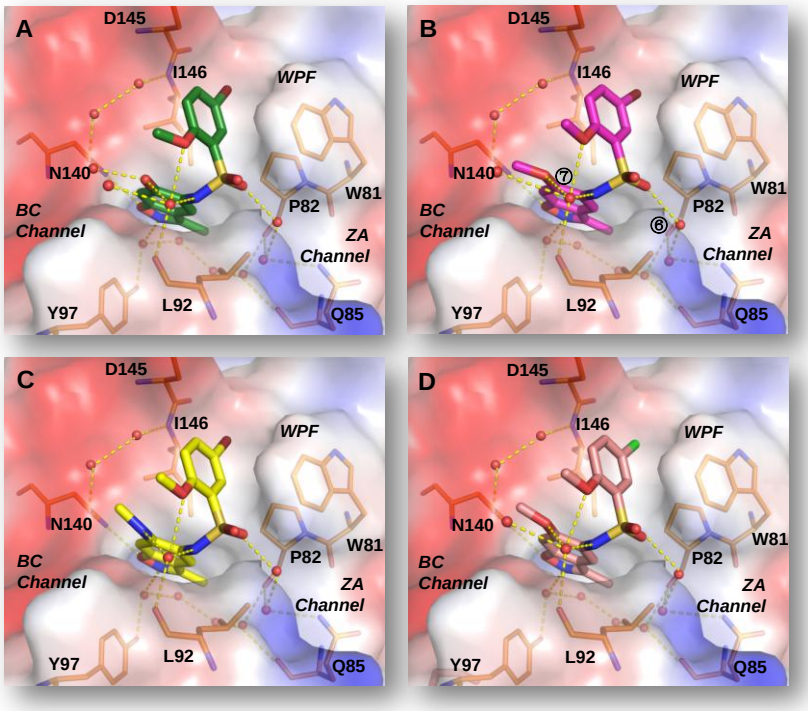

Figure 4. X-ray crystal structures of identified inhibitors in complex with BRD4(1). (A) **6a**–BRD4(1) (PDB ID: 5Y8W, carbon: green). (B) **6i**–BRD4(1) (PDB ID: 5Y8Y, carbon: magenta). (C) **6j**–BRD4(1) (PDB ID: 5Y94, carbon: yellow). (D) **6m**–BRD4(1) (PDB ID: 5Y8C, carbon: pink). Structures are shown with an electrostatic potential surface view.

To validate the importance of the 6-OCH_3 substitution, analogs of compound **6i** were prepared with various R^1 groups. Based on above established SAR from Table 1, representative R^1 groups acceptable for the WPF shelf were selected. The resulting compounds **6k–6n** exhibited a thermal

shift of over 7 °C and IC_{50} values ranging from 0.16 to 0.47 μM. They were more active than the corresponding 6-CH_3-substituted compounds **5k**, **5p**, **5s** and **5u**. Replacement of 5-bromo (**6i**) with 5-chloro (**6m**) on the phenyl ring led to a slightly decreased activity. The chlorine's smaller size may form weaker Van der Waals interaction with the hydrophobic WPF shelf (Figure 4D, Supporting Information, Figure S2).

2.1.4. SAR Studies of the Benzimidazole Derivatives.

Even though the sulfonamide derivatives exhibited good activities in the AlphaScreen and TSA assays, more chemotypes are needed to explore the therapeutic potential of BET inhibition for CRPC. In the above section, we demonstrated that the angle of the sulfonamide linker is important and ensure that the attached substituents occupy the WPF shelf. To reduce the molecular flexibility, a cyclization strategy was used at the sulfonamide position to maintain the similar angle and key binding characteristic. By searching literatures and patents, we found that a conformation restrained benzimidazole template was used as body of BRD4 inhibitors. Several patents from Boehringer Ingelheim[32-34] and GlaxoSmithKline[35] described that benzimidazole derivatives with a pyridone or bicyclic triazole as the acetyl lysine mimic can function as BRD4 inhibitors. Two structurally related benzimidazoles or bioisosteres of benzimidazoles reported by Engelhardt in the patents are exemplified in Supporting Information, Figure S3.[33,34] To investigate whether the benzo[*d*]isoxazole may act as an effective KAc mimic in structurally more diverse BRD4 inhibitors, we tried to introduce the benzimidazole template to the benzo[*d*]isoxazole scaffold using a hybridization strategy. Thus, novel benzimidazole-containing benzo[*d*]isoxazole derivatives were designed and synthesized.

Table 3. Structure−Activity Relationships of Compounds **7a−7n** for BRD4(1) Activities[a]

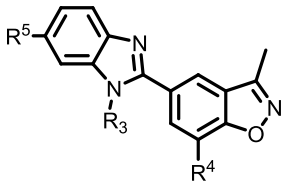

No.	R^3	R^4	R^5	TSA ΔT_m (°C)	AlphaScreen (μM)
7a		H		6.5	1.37 ± 0.78
7b		Br		6.2	1.80 ± 0.07
7c		H		5.9	1.16 ± 0.05
7d		Br		7.2	0.52 ± 0.04
7e	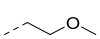	H		5.0	4.42 ± 0.72
7f	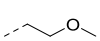	Br		4.5	>20
7g		H		6.5	1.41 ± 0.80
7h		Br		6.0	2.36 ± 0.45
7i		H		4.8	3.62 ± 0.24
7j	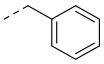	H		6.0	1.67 ± 0.36
7k	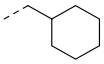	H		5.4	0.18 ± 0.02
7l	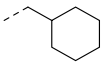	Br		9.2	0.30 ± 0.06
7m	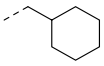	H		9.9	0.18 ± 0.01
7n	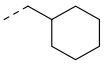	Br		7.2	0.32 ± 0.04

[a]The IC_{50} of all compounds in the table were calculated from at least two independent experiments. Values are given as the mean ± SD.

To investigate the possible binding mode, the designed compound **7a** (Table 3) was first docked into the bromodomain of BRD4(1) using the **6i**-BRD4(1) complex structure (PDB ID: 5Y8Y) as a template. The predicted binding mode indicated that compound **7a** bound snugly in the acetyl lysine binding pocket (Figure 5A). The benzo[*d*]isoxazole scaffold in **7a** adopted the same binding mode with that of **6i**. The benzimidazole nitrogen atom attached substituent stretched to the WPF shelf, and another nitrogen atom formed a hydrogen bond with the 6th water in the ZA channel. The planar benzimidazole group formed π-π interaction with residue Trp81. The morpholine, a commonly used group that was also adopted by Boehringer Ingelheim's patents,[33,34] extended to the solvent region outside the binding pocket. Based on the above analysis, we synthesized a series of benzimidazole-containing benzo[*d*]isoxazole derivatives and performed extensive SAR studies (Table 3).

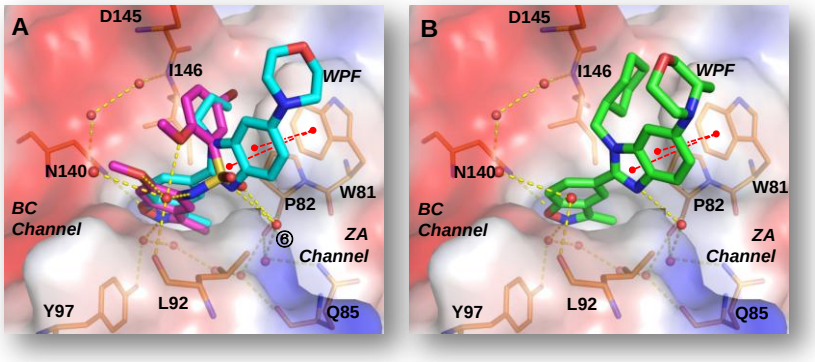

Figure 5. (A) Overlaid structures of compounds **6i** (PBD ID: 5Y8Y, carbon: magenta) and **7a** (docked pose, carbon: cyan) in complex with BRD4(1). (B) The docked pose of compound **7m** (carbon: green) in the BRD4(1) crystal structure (PDB ID: 5Y8Y).

We initially introduced a hydrophobic propyl group (**7a**) at the R^3 position of the benzimidazole to occupy the WPF shelf. **7a** demonstrated moderate potency against BRD4(1), with a ΔT_m value of 6.5 °C and an IC_{50} value of 1.37 μM. We further investigated the contribution of the R^3 group to BRD4(1) binding potencies. Inspired by the substituents in previous work,[23,33,34] the hydrophobic groups such as flexible alkyl or cycloalkyls with 3–4 heavy atoms and benzyl group were introduced at R^3 position. The resulting compounds **7b–7j** displayed comparable BRD4(1) binding potencies to compound **7a**. The investigation also revealed that a Br substitution was tolerated at the R^4 position. However, the effect of the Br substitution was sometimes beneficial to BRD4(1) activity (e.g. **7c** and **7d**), and sometimes detrimental (e.g. **7a** and **7b**; **7e** and **7f**; **7g** and **7h**). When a newly designed cyclohexylmethyl group was introduced at R^3 position, the resulting compounds **7k** and **7l** demonstrated improvement in their potencies with IC_{50} values of 0.18 and 0.30 μM against BRD4(1), respectively. Finally, the morpholine ring in the solvent region was replaced with a chiral (S)-3-methylmorpholine group (**7m** and **7n**), and comparable affinities were obtained.

To understand the possible binding mode of **7m** to BRD4(1), molecular docking was performed using the X-ray crystal structure of **6i**-BRD4(1) complex (PDB ID: 5Y8Y). The cyclohexylmethyl group of **7m** occupied the WPF shelf and formed extensive Van der Waals interactions with the hydrophobic residues Trp81, Pro82, and Ile146 (Figure 5B). The benzimidazole nitrogen atom formed a hydrogen bond with the 6th water in ZA channel, anchoring the benzimidazole group in a reasonable binding pose (Figure 5B). Taken together, the benzo[*d*]isoxazole scaffold is an effective KAc mimic for designing BET inhibitors.

2.2. Evaluation of the ITC Binding Affinities and Bromodomain Selectivity.

The most potent compounds from the two series were chosen for binding affinity determination using isothermal titration calorimetry (ITC) (Table 4, Figure 6A, 6B and Supporting Information, Figure S4). All the tested compounds displayed high potencies with K_d < 200 nM, which further validated their strong binding affinities to BRD4(1). Compounds **6i** and **7m** bound to the BRD4(1) bromodomain with K_d values of 82 and 81 nM, respectively. Overall, the results indicated that compounds **6i** and **7m** displayed comparable binding activities to that of reference compound **1**.

Table 4. ITC Determination of K_d for the Binding of the Representative Compounds to BRD4(1)

No.	K_d (nM)	N	ΔH (kcal/mol)	TΔS (kcal/mol)	ΔG (kcal/mol)
1	92	1.09	-9.3	0.32	-9.6
6i	82	0.96	-12.2	-2.5	-9.7
6j	164	0.95	-15.3	-6.0	-9.3
7l	159	1.02	-10.7	-1.4	-9.3
7m	81	1.18	-11.9	-2.2	-9.7

To investigate the selectivity profile, representative compounds were assessed by thermal stability shift assay against the 12 representative bromodomain-containing proteins BRD4(1), BRD2(1), BRD3(1), BRDT(1), BAZ2B, BRD1, BRD9, PCAF, TAF1(1), ASH1L, EP300 and CREBBP. Most of the compounds showed good selectivity for the BET bromodomains over other tested bromodomain-containing proteins (Figure 6C). For BRD4(1) protein, the thermal shifts for all the tested compounds were over 9 ℃. The sulfonamide derivatives **6i**, and **6j** displayed weak activities for PCAF, EP300, and CREBBP, with thermal shifts less than 2.7 ℃.

As **6j** displayed thermal shift of 2.3 ℃ against EP300, it was selected as a surrogate to validate the binding affinity using ITC assay. The ITC result showed that no detectable binding affinity of **6j** to EP300 was observed, which further demonstrated the good selectivity (Supporting Information, Figure S4D). The benzimidazole derivatives **7l** and **7m** exhibited excellent selectivity profiles for BET bromodomains over the other non-BET bromodomain-containing proteins in the TSA assays.

To further confirm the selectivity profile from our TSA result, these two most potent BET inhibitors **6i** and **7m** were also assessed by the commercial BROMOscan (DiscoverX) platform to give a clearer indication of selectivity. The assay was performed in 32 representative bromodomain modules at 5 μM concentration. BROMOscan profiling further confirmed the excellent selectivity of both compounds for BET bromodomain over other bromodomain subfamilies (Figure 6D and 6E, Supporting Information, Table S2).

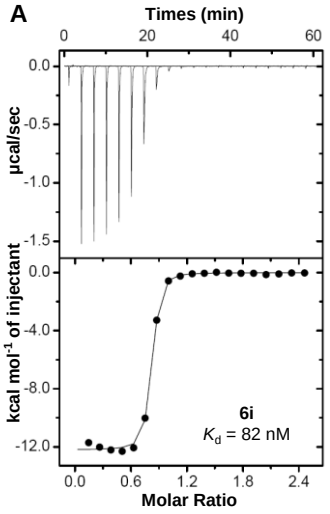

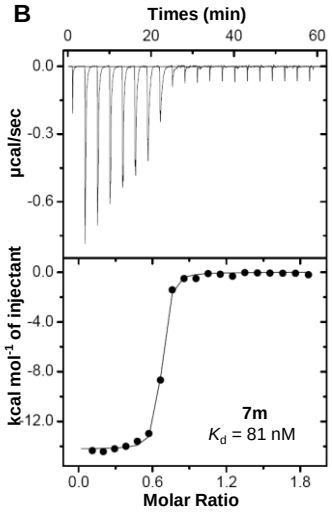

C

CPD	1	6i	6j	7l	7m
BRD4(1)	11.5	9.8	9.2	9.2	9.9
BRD2(1)	8.7	5.3	5.3	6	6.3
BRD3(1)	11	8.1	6.5	8.9	8.7
BRDT(1)	6.6	5.6	5.1	4.2	3.6
BAZ2B	-0.3	0	0.3	-0.6	-0.6
BRD1	0.5	-0.1	-0.4	0	0.3
BRD9	-1	-0.9	-0.8	-0.9	-0.8
PCAF	-0.1	2.7	2.6	-0.6	-0.6
TAF1(1)	-1	0.1	-0.1	-0.6	-0.9
ASH1L	-1	0.3	-0.1	-0.9	-0.5
EP300	-0.4	2	2.3	-0.3	0.3
CREBBP	-0.6	1.4	2.1	0	0.3

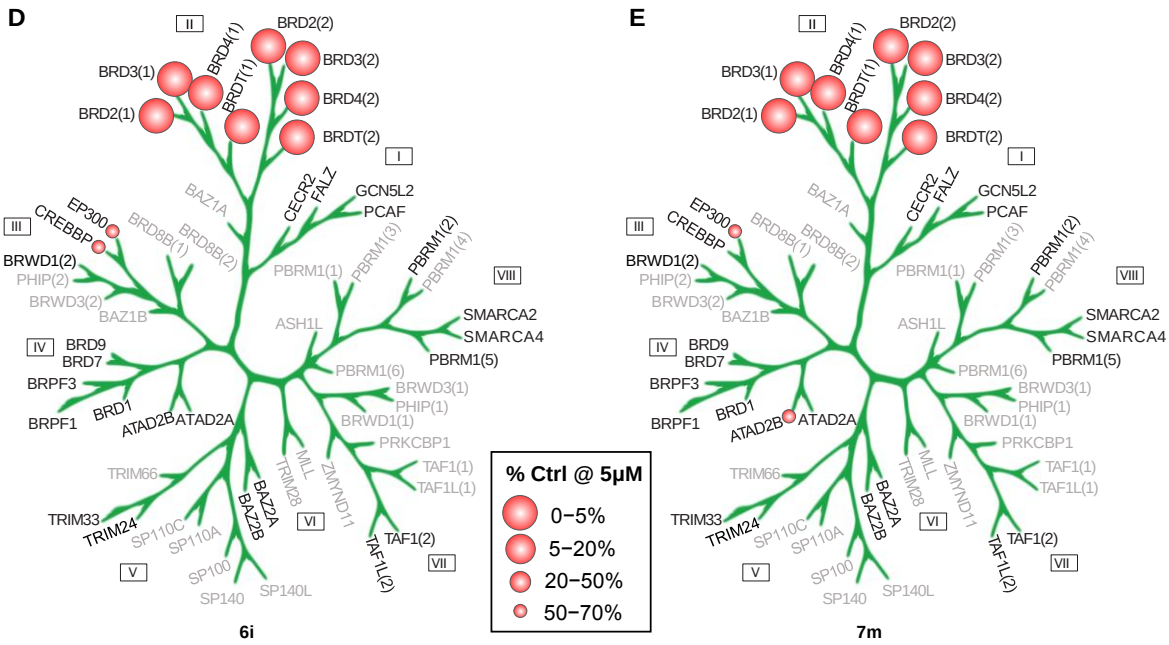

Figure 6. Determinations of binding affinities and bromodomain selectivity. (A, B) ITC titration curves for the binding of BRD4(1) to representative compounds **6i** (A) and **7m** (B). (C) Thermal shift analysis for selected compounds against twelve proteins from seven distinct BRD sub-families. The heat map shows the relative ΔT_m, where red indicates a large ΔT_m and yellow and green indicate small ΔT_m values. (D, E) Bromodomain selectivity profile of compounds **6i** (D) and **7m** (E) assessed by the BROMOscan (DiscoverX) platform at 5 μM concentration. The %Ctrl = (test compound signal − positive control signal) / (negative control signal − positive control signal) × 100%.

2.3. Evaluation of the Inhibitory Effects on Cell Growth, Gene and Protein Expression in Prostate Cancer Cells.

Given their high potencies and encouraging selectivity at the protein level, representative compounds were assessed for their inhibitory effects on cell growth in a panel of human prostate cancer cell lines such as LNCaP, C4-2B, 22Rv1 and VCaP (Figure 7). All the tested compounds

exhibited reasonable potencies in these cell lines. The compounds **6i**, **7l** and **7m** exhibited low micromolar or nanomolar potencies (IC_{50}: 0.29–2.6 μM) in the four AR-positive prostate cancer cell lines LNCaP, C4-2B, 22Rv1 and VCaP. All the tested BET inhibitors were less potent than compound **1** but more effective than second generation anti-androgen Enz in inhibiting cell growth, demonstrating the promising therapeutic potential of BET inhibition on CRPC.

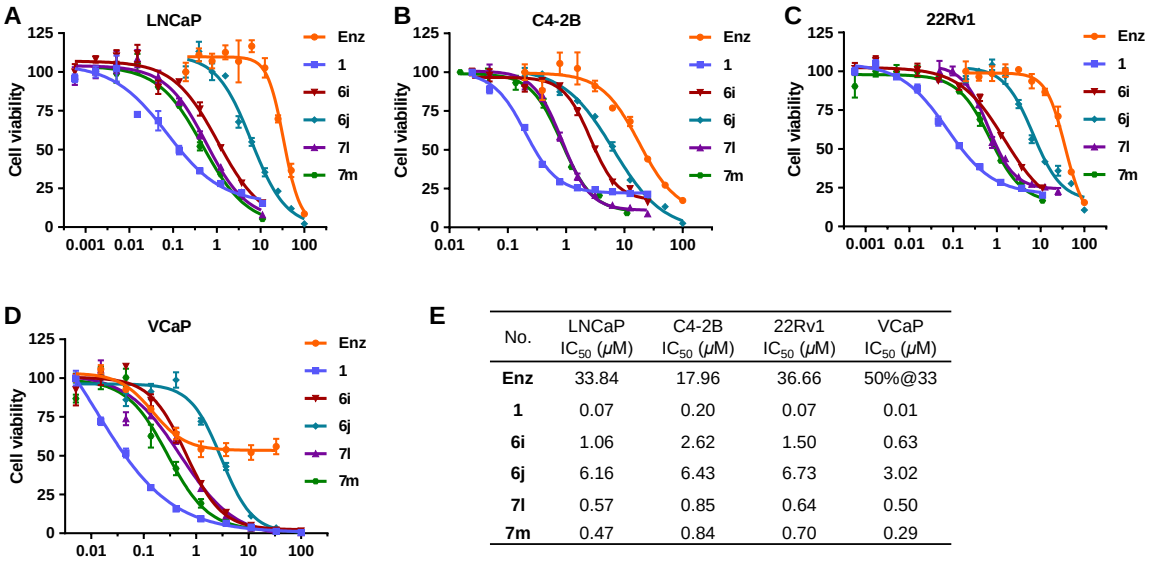

E

No.	LNCaP IC_{50} (μM)	C4-2B IC_{50} (μM)	22Rv1 IC_{50} (μM)	VCaP IC_{50} (μM)
Enz	33.84	17.96	36.66	50%@33
1	0.07	0.20	0.07	0.01
6i	1.06	2.62	1.50	0.63
6j	6.16	6.43	6.73	3.02
7l	0.57	0.85	0.64	0.50
7m	0.47	0.84	0.70	0.29

Figure 7. Cell viability, as measured by Cell-Titer GLO (Promega) of LNCaP (A), C4-2B (B), 22Rv1 (C) and VCaP (D) prostate cancer cells treated with the indicated concentrations of Enz, **1**, **6i**, **6j**, **7l**, and **7m**. Experiments were performed triplicate. (E) Half-maximum inhibitory concentration (IC_{50}) values for all compounds in each cell line are shown.

To evaluate cytotoxicity for various cell lines, compounds **6i** and **7m** were also evaluated in a wide range of cancer cell lines and normal cell lines (Supporting Information, Figure S5). Comparing with the AR-positive prostate cancer cell lines, **6i** and **7m** were less potent in AR-negative prostate cancer cells DU145 (IC_{50} > 6 μM) and PC-3 (IC_{50} > 3 μM). The inhibitory

effects of **6i** and **7m** in the AR-positive and AR-negative prostate cancer cell lines are consistent with that of compound **1** reported by Asangani et al.[12] Besides, the breast cancer cells MCF-7 and Hs578T also appeared to be sensitive to these compounds (IC_{50}: 1–2.5 μM). BET bromodomain inhibitors have previously shown antiproliferative effects in the AML MV4;11 cell line and human colon cancer HT-29 cell line reported by us and others.[10,11,23,37,38] Thus, it was not surprising to see that **6i** and **7m** demonstrated good inhibitory effect in MV4;11 and HT-29 (0.4–1.7 μM). The studies showed that **6i** and **7m** displayed moderate (2.5–5 μM) or weak (> 5 μM) inhibitory effects in the rest of cancer cell lines. Compound **1** is a widely used probe and exhibited stronger anti-proliferative effects in a range of cell lines compared to our compounds (Supporting Information, Figure S5). However, in our cellular assay (Figure S5), **1** exhibited very potent activities both in the cancer cell lines and in the normal lung fibroblast cell line HFL-1 (IC_{50} = 0.29 μM). Our compounds **6i** and **7m** exhibited weak cytotoxicity in the normal lung fibroblast cell line HFL-1 with IC_{50} values of 18.2 and 15.9 μM for **6i** and **7m**, respectively. Overall, the compounds showed preference for both acute leukemia cell lines such as MV4;11 and the AR-positive prostate cancer cell lines.

To evaluate the long term cell growth inhibitory effects, colony formation assays were conducted for the representative inhibitors **6i** and **7m**. Consistent with the cell viability assays, treatment of C4-2B and 22Rv1 cells with **6i** or **7m** reduced colony formations in a dose-dependent manner (Figure 8A). Colony formations were markedly suppressed by both compounds at 0.5 μM.

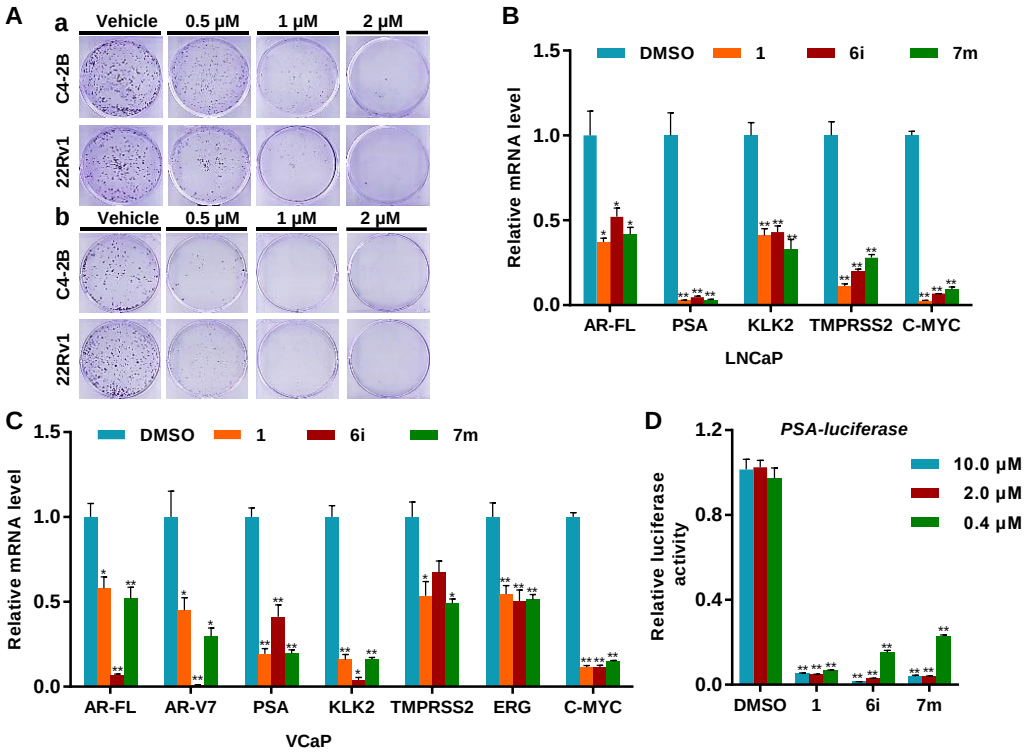

Figure 8. (A) Compounds **6i** (a) and **7m** (b) inhibit the colony formations of C4-2B and 22Rv1 prostate cancer cells. Cells were cultured and treated with vehicle (DMSO), 0.5 μM, 1.0 μM or 2.0 μM of **6i** or **7m** for 14 days followed by staining. (B, C) qRT-PCR analysis for mRNA expression in LNCaP cells (B) and VCaP cells (C) treated with vehicle (DMSO), **1** (5 μM), **6i** (5 μM) or **7m** (5 μM) for 48 h. (D) PSA transcriptional activity was evaluated by luciferase reporter assays in LNCaP cells transfected with PSA-luc reporter plasmid. Cells were treated with vehicle or with 0.4 μM, 2.0 μM or 10.0 μM of **1**, **6i** or **7m**. Data are expressed as the mean ± s.e.m. (n = 3). *$p < 0.05$ and **$p < 0.01$ by two-tailed Student's t-test.

qRT-PCR analysis was performed to explore whether the selected compounds would have an effect on AR, AR-regulated genes and other oncogenes expression in prostate cancer cells. As shown in Figure 8B and 8C, the AR-regulated genes KLK2, PSA (also known as KLK3) and

TMPRSS2 were suppressed at mRNA level upon **6i** or **7m** treatment in LNCaP and VCaP cells. MYC, a known oncogene in many types of cancer including prostate cancer, was previously identified as down-regulated by BET bromodomain inhibitors.[12,19,39,40] c-Myc mRNA level was significantly suppressed by **6i** or **7m** in both LNCaP and VCaP cells. ERG mRNA level was also suppressed upon **6i** or **7m** treatment in VCaP cells. Besides, the tested compounds suppressed the mRNA expression of full-length AR (AR-FL) or AR-V7 in VCaP cells. Furthermore, western blot analysis indicated that treatment of 22Rv1 cells with compounds **6i** and **7m** resulted in significant down regulation of both AR-FL and AR variants levels (Supporting Information, Figure S6).

As prostatic specific antigen (PSA) is currently the only recognized biomarker for the prostate cancer, a PSA promoter driven luciferase reporter assay was also designed as a surrogate to further evaluate the potential impact of compounds on transcription of PSA. Both **6i** and **7m** dose-dependently inhibited the PSA reporter activity and displayed comparable inhibitory effect to that of the reference BET inhibitor (**1**) (Figure 8D). The results suggested that the BET inhibitors **6i** and **7m** could effectively suppress cell growth and related gene expression in prostate cancer cells.

2.4. Pharmacokinetic Profiles of Compounds 6i and 7m.

The *in vivo* pharmacokinetic (PK) profiles were further evaluated for compounds **6i** and **7m**. Pharmacokinetic studies were performed after administering Sprague-Dawley (SD) rats with an intravenous (iv) dose of 2 mg/kg and an oral dose (po) of 10 mg/kg. As summarized in Table S3, after an iv administration, compound **6i** displays higher maximum concentration (C_{max} = 1392

μg/L) than that of **7m** (C_{max} = 807 μg/L). Both compounds exhibit reasonable exposure with AUC values of 1169 μg/L·h and 881 μg/L·h. It is disappointing that both compounds display poor drug exposure after an oral administration and results in low oral bioavailability. Compounds **6i** and **7m** may be further optimized to generate orally available candidates for drug development.

2.5. Compounds 6i and 7m Inhibit Prostate Cancer Tumor Growth.

We next evaluated the effects of compounds **6i** and **7m** on CRPC tumor growth using a C4-2B mouse xenograft model. Given the poor oral bioavailability, we adopted the intraperitoneal injection as the administration route. The mice were randomized and intraperitoneally (i.p.) treated with either vehicle or BET inhibitors **6i** or **7m** (50 mg/kg, five times per week) when the tumor volume was approximately 100 mm^3. The efficacy data showed that both **6i** and **7m** exhibited strong antitumor activities during the 25-day treatment period, with a tumor growth inhibition (TGI) of 70% and 51%, respectively (Figure 9A). Both compounds were well tolerated in the treated mice, based on the weight of the animal body and their general behavior (Figure 9B).

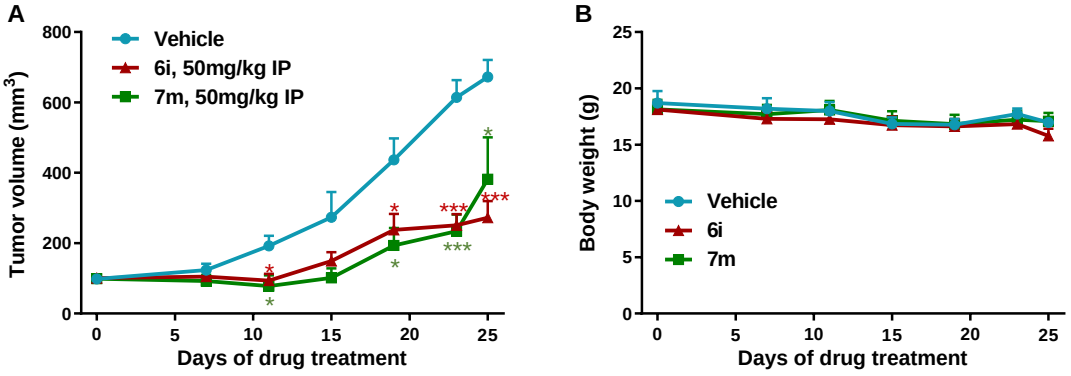

Figure 9. (A) Antitumor efficacy of compounds **6i** and **7m** in a C4-2B CRPC xenograft mouse model. (B) Body weight of mice during treatment with **6i** and **7m**. Mice were treated with intraperitoneal (i.p.) injections of vehicle or compounds **6i** and **7m** (50 mg/kg) five times per week. Data are expressed as the mean tumor volume ± s.e.m. of the animals in each treatment group. *$p < 0.05$, **$p < 0.01$, and ***$p < 0.001$ by two-tailed Student's t-test.

3. CHEMISTRY

The synthesis of novel benzo[*d*]isoxazole derivatives were illustrated in Schemes 1−4. In Scheme 1, commercially available **8a** was *N*-acetylated with acetic anhydride to give **9a**, which was converted to **10a** via a Friedel-Crafts reaction. Compound **10a** was used to prepare the oxime precursor **11a**, which was cyclized at high temperature to yield the benzo[*d*]isoxazole scaffold **12a**. Deprotection of the *N*-acetyl group of **12a** with dilute hydrochloric acid generated aniline **13a**. This was then capped with sulfonyl chlorides to give the sulfonamide derivatives **5a–5v**. The synthesis of compounds **6i** and **6k–6n** followed the same procedures as mentioned above with **8b** as the starting material.

In Scheme 2, the methyl group of the intermediate **13b** was removed using boron tribromide to afford compound **14**, which was further capped with sulfonyl chloride to give compound **6a**. O-alkylation of **6a** using different haloalkanes gave **6b**, **6g**, and **6h**. Subsequently, **6b** was hydrolyzed to acid **6c**, followed by coupling with available amines to obtain target compounds **6d–6f**.

In Scheme 3, the phenol derivative **15** was acetylated with acetic anhydride to afford compound **16**. This was then converted to **17** under $AlCl_3$-mediated Fries rearrangement conditions. The subsequent two steps were similar to Scheme 1, including oximation and cyclization, which furnished compound **19**. Treatment of **19** with fuming nitric acid gave the nitro-substituted compound **20**. **20** was then reacted with methylamine to afford the corresponding amine-substituted derivative **21**. Reduction and sulfonylation gave the target compound **6j**.

In Scheme 4, starting from commercially available **23**, the intermediate **25a** was obtained through a Fries rearrangement and an esterification reaction. Treatment of **25a** with bromine gave the Br-substituted compound **25b**. Next, **27a** and **27b** were prepared in two steps from **25a** and **25b**, respectively, following the same procedure as mentioned in Scheme 1. Deprotection of **27a** and **27b** gave the acid fragments **28a** and **28b**, respectively. Subsequently, 2-chloro-4-fluoro-1-nitrobenzene **29** was reacted with different amines in two steps to give the amine-substituted nitrobenzene intermediates **31a–31h**. Reduction of the nitro groups led to the corresponding anilines **32a–32h**, which were coupled with the acid **28a** or **28b**, followed by a ring closing reaction using acetic acid to give the final products **7a–7n**.

Scheme 1. Synthesis of sulfonamide derivatives **5a–5v**, **6i**, and **6k–6n**[a]

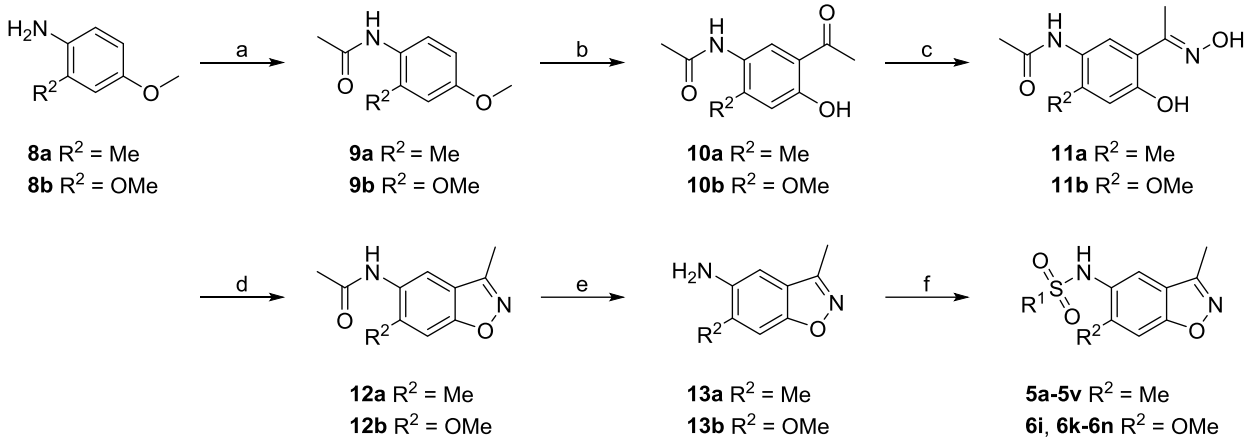

[a]Reagents and conditions: (a) acetic anhydride, Et_3N, CH_2Cl_2, rt, 68−71%; (b) acetyl chloride, $AlCl_3$, CH_2Cl_2, 0−43 °C, 78−80%; (c) NH_2-OH·HCl, NaOAc, EtOH/H_2O, 80 °C, 94−99%; (d) DMF-DMA, 1,4-dioxane, 100 °C, 61−70%; (e) HCl/H_2O, reflux, 96−97%; (f) R^1SO_2Cl, pyridine, CH_2Cl_2, reflux, 11−80%.

Scheme 2. Synthesis of O-linked R^2 derivatives **6a–6h**[a]

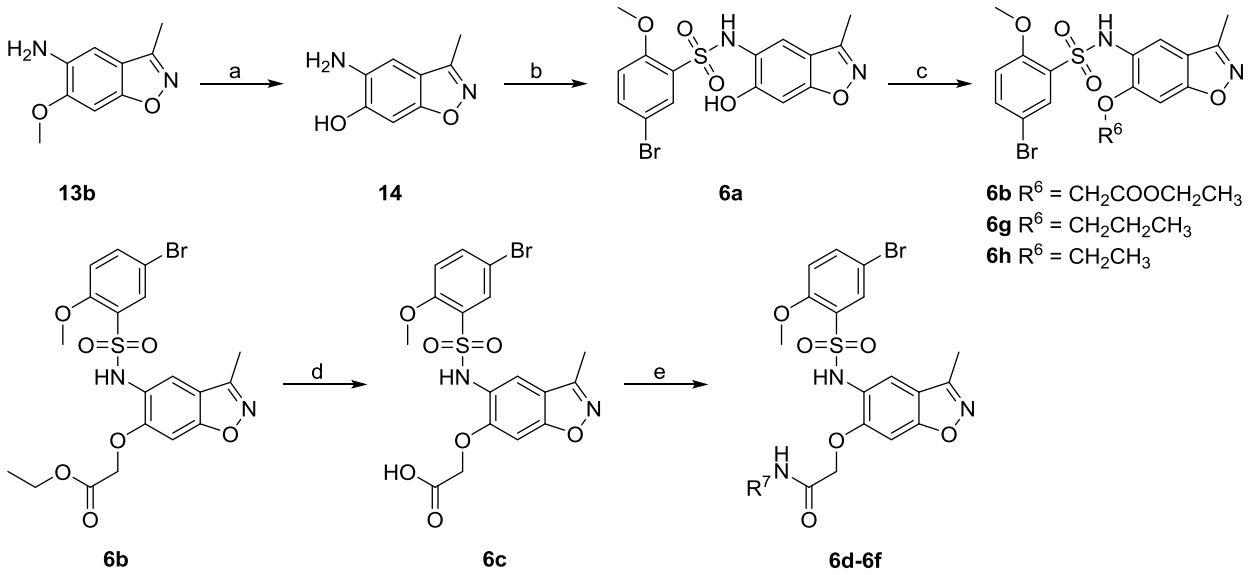

[a]Reagents and conditions: (a) BBr_3, CH_2Cl_2, rt, 91%; (b) 5-bromo-2-methoxybenzene sulfonyl chloride, pyridine, CH_2Cl_2, rt, 71%; (c) R^6X (X= Cl or I), K_2CO_3, KI, acetone, 50 °C, 31−33%; (d) NaOH, H_2O, MeOH, rt, 76%; (e) R^7NH_2, HATU, DIPEA, DMF, rt, 32−48%.

Scheme 3. Synthesis of N-linked R^2 derivative **6j**[a]

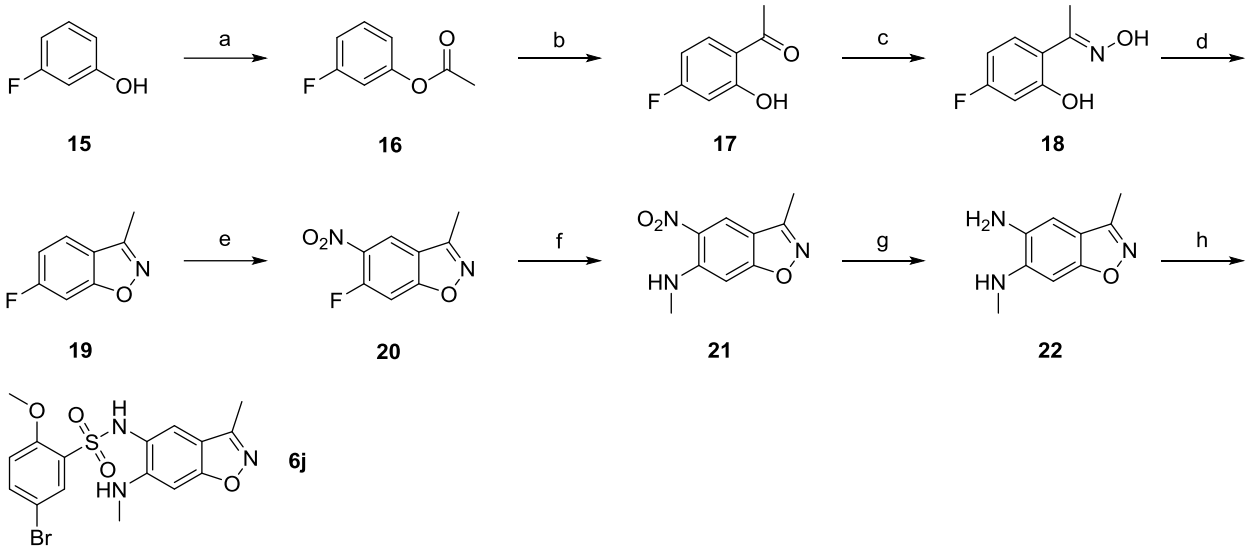

[a]Reagents and conditions: (a) acetic anhydride, H_2SO_4, CH_2Cl_2, rt, 76%; (b) $AlCl_3$, 190 ℃, 71%; (c) NH_2-OH·HCl, NaOAc, EtOH/H_2O, 80 ℃, 86%; (d) acetic anhydride, NaOAc, DMF, 100 ℃, 90%; (e) HNO_3, H_2SO_4, 0 ℃, rt, 82%; (f) CH_3NH_2, K_2CO_3, THF, 45 ℃, 95%; (g) $SnCl_2 \cdot 2H_2O$, HCl (conc.), acetic acid, 40 ℃, 39%; (h) 5-bromo-2-methoxybenzenesulfonyl chloride, pyridine, CH_2Cl_2, reflux, 71%.

Scheme 4. Synthesis of benzimidazole derivatives **7a–7n**[a]

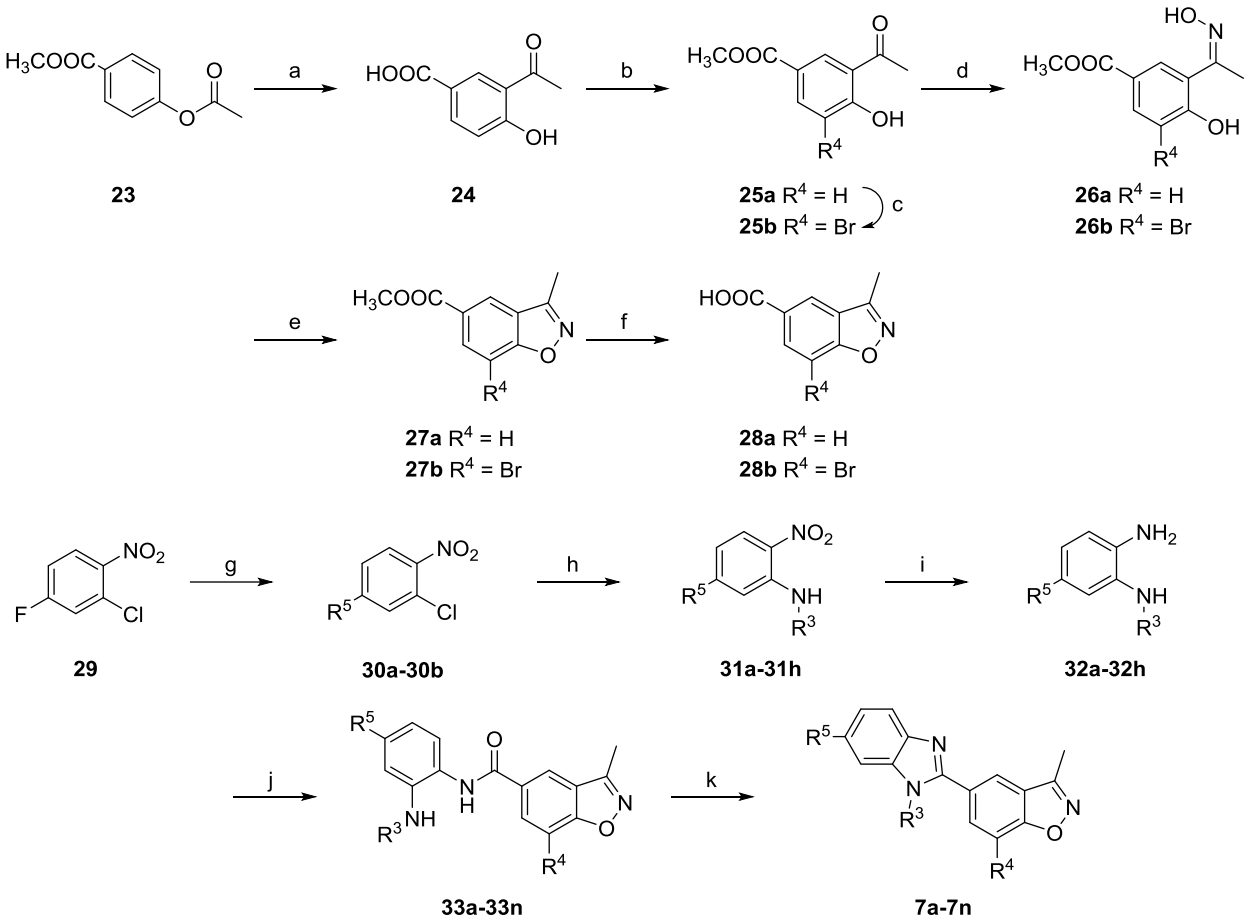

[a]Reagents and conditions: (a) $AlCl_3$, KCl, 170 ℃, 88%; (b) $SOCl_2$, MeOH, 0 ℃, reflux, 62%; (c) Br_2, pyridine, CH_2Cl_2, rt, 90%; (d) NH_2-OH·HCl, NaOAc, EtOH/H_2O, 78 °C, 85−92%; (e) DMF-DMA, 1,4-dioxane, 100 °C, 61−78%; (f) NaOH, H_2O, rt, 97−99%; (g) morpholine or (S)-3-methylmorpholine, K_2CO_3, DMF, 100 ℃, 97%; (h) R^3NH_2, DIPEA, DMSO, 95−120 ℃, 91%; (i) 10% Pd-C, H_2, MeOH/THF, rt; or Fe, AcOH, NH_4Cl, EtOH/H_2O, 80 ℃, 60−84%; (j) **28a** or **28b**, HATU, DIPEA, DMF, rt, 10−52%; or CMPI, tributylamine, toluene, 90 ℃, 14−46%; (k) AcOH, 120−150 °C, 11−60%.

4. CONCLUSIONS

In this study, we reported the structure-based design, synthesis, and evaluation of the benzo[*d*]isoxazole derivatives as a new class of selective BET bromodomain inhibitors. Determination of the high-resolution crystal structures provided guidance for the extensive structural optimization and resulted in potent BET inhibitors. The most promising compounds, **6i** and **7m**, strongly bound to BRD4(1) with K_d values of 82 and 81 nM, respectively. The compounds also potently inhibited cell growth, colony formation, and the expression of AR, AR regulated genes and MYC in prostate cancer cell lines. Compounds **6i** and **7m** exhibited promising therapeutic effects in a C4-2B CRPC mouse xenograft model. In summary, these data indicate that the promising compounds **6i** and **7m** may serve as new lead compounds for further optimization for treatment of CRPC.

5. EXPERIMENTAL SECTION

5.1. Docking Studies.

The crystal structures of BRD4(1) in complex with inhibitor **1** (PDB ID: 3MXF), **4** (PDB ID: 5DX4) and **6i** (PDB ID: 5Y8Y) were used as the reference structures. All the ligand and protein preparations were performed in Maestro (version 9.4, Schrödinger, LLC, New York, NY, 2013) implemented in the Schrödinger program. The proteins were prepared using the Protein Preparation Wizard within Maestro 9.4 (Schrödinger, LLC). The hydrogens were added, bond orders were assigned, and missing side chains for some residues were added using Prime. The added hydrogens were subjected to energy minimization until the root-mean-square deviation (RMSD) relative to the starting geometry reached 0.3 Å. The Glide docking program in Maestro 9.4 was used for docking studies. For Glide docking, the grid was defined using a 20 Å box

centered on the ligand, and the important water molecules around ligand were kept. All parameters were kept as default. The designed molecules were docked using Glide SP mode, and the predicted binding poses of all the compounds were ranked according to their glidescores.

5.2. General Chemistry. All the commercial reagents were used without further purification unless otherwise specified. Final compounds were purified either by silica gel chromatography (300-400 mesh) or by recrystallization. ^{1}H-NMR and ^{13}C-NMR spectra were recorded on Bruker AV-400 or AV-500 spectrometer. Coupling constants (*J*) are expressed in hertz (Hz). NMR chemical shifts (δ) are reported in parts per million (ppm) units relative to the internal control (TMS). The ESI-MS were recorded on an Agilent 1200 HPLC-MSD mass spectrometer. The compound purity was determined by reverse-phase high-performance liquid chromatography (HPLC) with 20% solvent A (H_2O) and 80% solvent B (MeOH or 0.5‰ NH_3 in MeOH) as eluents. HPLC analysis use a Dionex Summit HPLC column (Inertsil ODS-SP, 5.0 μm, 4.6 mm × 250 mm (GL Sciences Inc.)) with a UVD170U detector, and a manual injector, a P680 pump with a detection wavelength of 254 nm and a flow rate of 1.0 mL/min. The purity of all the final compounds was determined by HPLC to be >95%.

***N*-(3,6-Dimethylbenzo[*d*]isoxazol-5-yl)ethanesulfonamide (5a).**

Step 1: 4-Methoxy-2-methylaniline (**8a**, 10.0 g, 72.9 mmol) and Et_3N (11.8 g, 116.6 mmol) were dissolved in CH_2Cl_2. Acetic anhydride (9.7 mL, 102.1 mmol) was then added to the mixture under ice-cooling. The mixture was stirred at 0 ℃ for 2 h. Then, 10% aqueous citric acid solution was added to the reaction mixture. The mixture was extracted with EtOAc. The organic layer was washed with 1 N HCl, saturated $NaHCO_3$ solution and brine. The separated organic

phase was dried over Na_2SO_4 and concentrated under reduced pressure. The crude product was washed with petroleum ether and dried to give *N*-(4-methoxy-2-methylphenyl)acetamide (**9a**) as a pale-pink solid (8.9 g, 68% yield). ^{1}H NMR (500 MHz, DMSO-d_6) δ 9.16 (s, 1H), 7.18 (d, J = 8.7 Hz, 1H), 6.77 (d, J = 2.7 Hz, 1H), 6.70 (dd, J = 8.7, 2.8 Hz, 1H), 3.71 (s, 3H), 2.14 (s, 3H), 2.00 (s, 3H). MS (ESI) *m/z* $[M + H]^+$ calcd 180.09; found 180.0.

Step 2: Compound **9a** (8.9 g, 49.6 mmol) was dissolved in CH_2Cl_2 (40 mL). Acetyl chloride (11.7 g, 148.8 mmol) and aluminum chloride (26.5 g, 198.4 mmol) were added successively under ice-cooling with stirring and the mixture was heated under reflux for 2 h. The reaction mixture was cooled, poured into ice water, stirred for 2 h and extracted with CH_2Cl_2. The organic layer was washed with brine, dried over Na_2SO_4 and concentrated under reduced pressure. The crude product was washed with petroleum ether to give *N*-(5-acetyl-4-hydroxy-2-methylphenyl)acetamide (**10a**) as a brick-red solid (8.2 g, 80% yield). ^{1}H NMR (400 MHz, DMSO-d_6) δ 11.80 (s, 1H), 9.31 (s, 1H), 7.77 (s, 1H), 6.83 (s, 1H), 2.57 (s, 3H), 2.19 (s, 3H), 2.03 (s, 3H). MS (ESI) *m/z* $[M + H]^+$ calcd 208.09; found 208.0.

Step 3: To an EtOH−H_2O mixed solvent (3:1, 160 mL) was added compound **10a** (8.0 g, 38.6 mmol), hydroxylamine hydrochloride (4.3 g, 61.8 mmol) and NaOAc (5.0 g, 61.8 mmol). The mixture was heated under reflux for 70 min. The reaction mixture was cooled and concentrated under reduced pressure to allow precipitation of the solid. Water (50 mL) was added, and the precipitated solid was filtered, washed and dried to give *N*-(4-hydroxy-5-(1-(hydroxyimino)ethyl)-2-methylphenyl)acetamide (**11a**) as a pale red solid (8.5 g, 99% yield). ^{1}H NMR (400 MHz, DMSO-d_6) δ 11.49 (s, 1H), 11.37 (s, 1H), 9.22 (s, 1H), 7.34 (s, 1H), 6.72 (s, 1H), 2.19 (s, 3H), 2.12 (s, 3H), 2.01 (s, 3H).

Step 4: To a solution of compound **11a** (8.5 g, 38.3 mmol) in 1,4-dioxane (25 mL) was added DMF-DMA (23 mL) with vigorous stirring. The mixture was stirred with heating at 100 ℃ for 7 min. The reaction mixture was cooled and extracted with EtOAc. The organic layer was washed with brine, dried over Na_2SO_4, and concentrated under reduced pressure to give *N*-(3,6-dimethylbenzo[*d*]isoxazol-5-yl)acetamide (**12a**) as a brown solid (4.8 g, 61% yield). ^{1}H NMR (400 MHz, DMSO-d_6) δ 9.41 (s, 1H), 7.77 (s, 1H), 7.56 (s, 1H), 2.50 (s, 3H), 2.35 (s, 3H), 2.09 (s, 3H). MS (ESI) *m/z* $[M + H]^+$ calcd 205.09; found 205.0.

Step 5: To the product **12a** (4.8 g, 23.5 mmol) was added 3 N HCl (100 mL). The mixture was heated under reflux for 2 h. Upon completion of the reaction, the mixture was cooled to 0 °C and basified to pH 7−9 with NaOH solution. The precipitated solid was collected by filtration, washed with water and dried to give 3,6-dimethylbenzo[*d*]isoxazol-5-amine (**13a**) as a brown solid (3.7 g, 97% yield). ^{1}H NMR (400 MHz, DMSO-d_6) δ 7.29 (s, 1H), 6.83 (s, 1H), 4.89 (brs, 2H), 2.41 (s, 3H), 2.21 (s, 3H). MS (ESI) *m/z* $[M + H]^+$ calcd 163.08; found 163.0.

Step 6: To a solution of **13a** (50 mg, 0.31 mmol) in CH_2Cl_2 (5 mL) were added ethanesulfonyl chloride (59.1 mg, 0.46 mmol) and pyridine (1 mL). The mixture was stirred at 45 ℃ for 2 h. The reaction mixture was extracted with CH_2Cl_2 and washed with 1 N HCl and brine. The organic layer was dried over Na_2SO_4 and concentrated under reduced pressure. The residue was purified by silica gel chromatography to give the title compound **5a** as a white solid (35 mg, 45% yield). ^{1}H NMR (400 MHz, DMSO-d_6) δ 9.19 (s, 1H), 7.66 (s, 1H), 7.60 (s, 1H), 3.16 (q, J = 7.3 Hz, 2H), 2.53 (s, 3H), 2.47 (s, 3H), 1.28 (t, J = 7.3 Hz, 3H). ^{13}C NMR (126 MHz, $CDCl_3$) δ 161.2, 155.2, 134.7, 131.1, 121.6, 116.0, 111.6, 46.9, 19.5, 10.3, 8.4. MS (ESI) *m/z* $[M + H]^+$ calcd 255.07; found 255.0. HPLC, t_R = 4.70 min, 98.15% purity.

***N*-(3,6-Dimethylbenzo[*d*]isoxazol-5-yl)propane-1-sulfonamide (5b).** Compound **5b** was prepared from **13a** and propane-1-sulfonyl chloride according to general procedure of step 6 as described for **5a**. White solid, 39% yield. ^{1}H NMR (400 MHz, DMSO-d_6) δ 9.20 (s, 1H), 7.65 (s, 1H), 7.60 (s, 1H), 3.17 – 3.08 (m, 2H), 2.53 (s, 3H), 2.46 (s, 3H), 1.82 – 1.69 (m, 2H), 1.00 (t, J = 7.4 Hz, 3H). ^{13}C NMR (126 MHz, $CDCl_3$) δ 161.2, 155.2, 134.6, 131.1, 121.6, 115.9, 111.6, 54.3, 19.5, 17.5, 13.1, 10.3. MS (ESI) *m/z* $[M + H]^+$ calcd 269.09; found 269.0. HPLC, t_R = 5.24 min, 98.11% purity.

***N*-(3,6-Dimethylbenzo[*d*]isoxazol-5-yl)butane-1-sulfonamide (5c).** Compound **5c** was prepared from **13a** and butane-1-sulfonyl chloride according to general procedure of step 6 as described for **5a**. Light red solid, yield 46%. ^{1}H NMR (400 MHz, DMSO-d_6) δ 9.21 (s, 1H), 7.65 (s, 1H), 7.60 (s, 1H), 3.20 – 3.07 (m, 2H), 2.53 (s, 3H), 2.46 (s, 3H), 1.81 – 1.63 (m, 2H), 1.51 – 1.33 (m, 2H), 0.89 (t, J = 7.3 Hz, 3H). ^{13}C NMR (126 MHz, $CDCl_3$) δ 160.5, 155.1, 138.7, 131.8, 120.4, 119.4, 110.6, 51.7, 25.2, 20.8, 19.2, 13.5, 9.6. MS (ESI) *m/z* $[M + H]^+$ calcd 283.10; found 283.0. HPLC, t_R = 6.02 min, 99.18% purity.

***N*-(3,6-Dimethylbenzo[*d*]isoxazol-5-yl)cyclopentanesulfonamide (5d).** Compound **5d** was prepared from **13a** and cyclopentanesulfonyl chloride according to general procedure of step 6 as described for **5a**. White solid, 11% yield. ^{1}H NMR (400 MHz, DMSO-d_6) δ 9.18 (s, 1H), 7.66 (s, 1H), 7.59 (s, 1H), 3.64 (p, J = 7.6 Hz, 1H), 2.53 (s, 3H), 2.47 (s, 3H), 1.93 (d, J = 5.5 Hz, 4H), 1.72 – 1.63 (m, 2H), 1.62 – 1.53 (m, 2H). ^{13}C NMR (126 MHz, DMSO-d_6) δ 160.5, 155.1, 138.6, 132.0, 120.4, 119.2, 110.5, 60.8, 27.7 (2 × C), 25.5 (2 × C), 19.3, 9.6. MS (ESI) *m/z* $[M + H]^+$ calcd 295.10; found 295.0. HPLC, t_R = 6.07 min, 98.00% purity.

***N*-(3,6-Dimethylbenzo[*d*]isoxazol-5-yl)cyclohexanesulfonamide (5e).** Compound **5e** was prepared from **13a** and cyclohexanesulfonyl chloride according to general procedure of step 6 as described for **5a**. White solid, 29% yield. ^{1}H NMR (400 MHz, DMSO-d_6) δ 9.13 (s, 1H), 7.64 (s, 1H), 7.59 (s, 1H), 3.09 – 3.02 (m, 1H), 2.53 (s, 3H), 2.47 (s, 3H), 2.11 (d, J = 11.1 Hz, 2H), 1.79 (d, J = 12.7 Hz, 2H), 1.63 (d, J = 12.4 Hz, 1H), 1.49 – 1.37 (m, 2H), 1.35 – 1.26 (m, 2H), 1.22 – 1.08 (m, 1H). ^{13}C NMR (126 MHz, DMSO-d_6) δ 160.4, 155.1, 138.5, 132.1, 120.4, 119.2, 110.5, 60.2, 26.3 (2 × C), 24.9, 24.4 (2 × C), 19.3, 9.6. MS (ESI) *m/z* $[M - H]^-$ calcd 307.12; found 307.2. HPLC, t_R = 7.26 min, 98.05% purity.

***N*-(3,6-Dimethylbenzo[*d*]isoxazol-5-yl)benzenesulfonamide (5f).** Compound **5f** was prepared from **13a** and benzenesulfonyl chloride according to general procedure of step 6 as described for **5a**. White solid, 61% yield. ^{1}H NMR (400 MHz, DMSO-d_6) δ 9.75 (s, 1H), 7.66 (t, J = 7.2 Hz, 1H), 7.62 (d, J = 8.1 Hz, 2H), 7.54 (t, J = 7.6 Hz, 2H), 7.48 (s, 1H), 7.36 (s, 1H), 2.44 (s, 3H), 2.02 (s, 3H). ^{13}C NMR (126 MHz, $CDCl_3$) δ 161.6, 155.3, 139.6, 136.3, 133.3, 130.4, 129.3 (2 × C), 127.2 (2 × C), 121.5, 118.9, 111.2, 18.9, 10.2. MS (ESI) *m/z* $[M + H]^+$ calcd 303.07; found 303.0. HPLC, t_R = 5.74 min, 99.31% purity.

***N*-(3,6-Dimethylbenzo[*d*]isoxazol-5-yl)-4-fluorobenzenesulfonamide (5g).** Compound **5g** was prepared from **13a** and 4-fluorobenzenesulfonyl chloride according to general procedure of step 6 as described for **5a**. White solid, 57 % yield. ^{1}H NMR (400 MHz, DMSO-d_6) δ 9.82 (s, 1H), 7.67 (dd, J = 8.6, 5.3 Hz, 2H), 7.51 (s, 1H), 7.39 (t, J = 8.8 Hz, 2H), 7.38 (s, 1H), 2.46 (s, 3H), 2.05 (s, 3H). ^{13}C NMR (126 MHz, $CDCl_3$) δ 166.5, 164.5 (d, J = 257.0 Hz, 1C), 161.6, 155.2,

136.2, 135.7, 135.7 (d, J = 3.8 Hz, 1C), 130.1, 130.0, 130.0 (d, J = 10.1 Hz, 2C), 121.6, 119.0, 116.7, 116.5 (d, J = 22.7 Hz, 2C), 111.3, 18.9, 10.2. MS (ESI) *m/z* $[M + H]^+$ calcd 321.06; found 321.0. HPLC, t_R = 6.22 min, 99.32% purity.

4-Chloro-*N*-(3,6-dimethylbenzo[*d*]isoxazol-5-yl)benzenesulfonamide (5h). Compound **5h** was prepared from **13a** and 4-chlorobenzenesulfonyl chloride according to general procedure of step 6 as described for **5a**. White solid, 71% yield. ^{1}H NMR (400 MHz, DMSO-d_6) δ 9.88 (s, 1H), 7.74 – 7.57 (m, 4H), 7.51 (s, 1H), 7.40 (s, 1H), 2.46 (s, 3H), 2.05 (s, 3H). ^{13}C NMR (126 MHz, $CDCl_3$) δ 161.6, 155.2, 140.0, 138.1, 136.1, 130.0, 129.6 (2 × C), 128.7 (2 × C), 121.6, 119.0, 111.4, 19.0, 10.2. MS (ESI) *m/z* $[M + H]^+$ calcd 337.03; found 337.0. HPLC, t_R = 7.97 min, 99.28% purity.

***N*-(3,6-Dimethylbenzo[*d*]isoxazol-5-yl)-4-nitrobenzenesulfonamide (5i).** Compound **5i** was prepared from **13a** and 4-nitrobenzenesulfonyl chloride according to general procedure of step 6 as described for **5a**. White solid, 79% yield. ^{1}H NMR (400 MHz, DMSO-d_6) δ 10.19 (s, 1H), 8.38 (d, J = 8.6 Hz, 2H), 7.87 (d, J = 8.6 Hz, 2H), 7.53 (s, 1H), 7.42 (s, 1H), 2.46 (s, 3H), 2.06 (s, 3H). ^{13}C NMR (126 MHz, DMSO-d_6) δ 160.8, 155.0, 149.8, 145.8, 138.7, 130.3 (2 × C), 128.2, 128.1, 124.7, 120.5, 120.4, 110.7, 18.5, 9.5. MS (ESI) *m/z* $[M + H]^+$ calcd 348.06; found 348.0. HPLC, t_R = 6.25 min, 99.21% purity.

***N*-(3,6-Dimethylbenzo[*d*]isoxazol-5-yl)-4-methoxybenzenesulfonamide (5j).** Compound **5j** was prepared from **13a** and 4-methoxybenzenesulfonyl chloride according to general procedure of step 6 as described for **5a**. White solid, 71% yield. ^{1}H NMR (400 MHz, DMSO-d_6) δ 9.58 (s,

1H), 7.53 (d, J = 8.6 Hz, 2H), 7.48 (s, 1H), 7.38 (s, 1H), 7.05 (d, J = 8.6 Hz, 2H), 3.81 (s, 3H), 2.45 (s, 3H), 2.05 (s, 3H). ^{13}C NMR (126 MHz, DMSO-d_6) δ 162.4, 160.5, 154.9, 138.5, 131.9, 131.2, 128.8 (2 × C), 120.3, 119.9, 114.3 (2 × C), 110.4, 55.6, 18.5, 9.4. MS (ESI) m/z $[M + H]^+$ calcd 333.08; found 333.0. HPLC, t_R = 6.08 min, 99.74% purity.

2-Chloro-*N*-(3,6-dimethylbenzo[*d*]isoxazol-5-yl)benzenesulfonamide (5k). Compound **5k** was prepared from **13a** and 2-chlorobenzenesulfonyl chloride according to general procedure of step 6 as described for **5a**. White solid, 78% yield. ^{1}H NMR (400 MHz, DMSO-d_6) δ 10.06 (s, 1H), 7.80 (d, J = 7.8 Hz, 1H), 7.72 (d, J = 7.8 Hz, 1H), 7.66 (t, J = 7.6 Hz, 1H), 7.52 (s, 1H), 7.45 (t, J = 7.6 Hz, 1H), 7.36 (s, 1H), 2.42 (s, 3H), 2.22 (s, 3H). ^{13}C NMR (126 MHz, DMSO-d_6) δ 160.7, 154.9, 139.1, 137.9, 134.4, 131.9, 130.9, 130.8, 130.6, 127.7, 120.4, 120.3, 110.5, 18.5, 9.4. MS (ESI) m/z $[M + H]^+$ calcd 337.03; found 337.0. HPLC, t_R = 6.27 min, 100.00% purity.

2-Bromo-*N*-(3,6-dimethylbenzo[*d*]isoxazol-5-yl)benzenesulfonamide (5l). Compound **5l** was prepared from **13a** and 2-bromobenzenesulfonamide according to general procedure of step 6 as described for **5a**. White solid, 63% yield. ^{1}H NMR (400 MHz, DMSO-d_6) δ 10.02 (s, 1H), 7.90 (d, J = 7.7 Hz, 1H), 7.84 (d, J = 7.6 Hz, 1H), 7.55 (t, J = 7.5 Hz, 1H), 7.52 (s, 1H), 7.49 (t, J = 7.4 Hz, 1H), 7.35 (s, 1H), 2.42 (s, 3H), 2.23 (s, 3H). ^{13}C NMR (126 MHz, DMSO-d_6) δ 160.7, 154.9, 139.5, 139.1, 135.4, 134.3, 131.2, 130.6, 128.2, 120.3, 120.3, 119.4, 110.5, 18.6, 9.4. MS (ESI) m/z $[M + H]^+$ calcd 380.98 & 382.98; found 380.9 & 382.9. HPLC, t_R = 6.79 min, 98.93% purity.

Methyl 2-(*N*-(3,6-dimethylbenzo[*d*]isoxazol-5-yl)sulfamoyl)benzoate (5m). Compound **5m** was prepared from **13a** and methyl 2-(chlorosulfonyl)benzoate according to general procedure of step 6 as described for **5a**. White solid, 86% yield. ^{1}H NMR (400 MHz, DMSO-d_6) δ 9.50 (s, 1H), 7.76 – 7.69 (m, 1H), 7.67 – 7.60 (m, 3H), 7.50 (s, 1H), 7.48 (s, 1H), 3.69 (s, 3H), 2.47 (s, 3H), 2.08 (s, 3H). ^{13}C NMR (126 MHz, DMSO-d_6) δ 167.5, 160.7, 155.0, 138.8, 137.6, 133.0, 131.8, 130.9, 130.7, 128.8, 128.6, 120.4, 120.4, 110.4, 52.8, 18.3, 9.4. MS (ESI) *m/z* $[M + H]^+$ calcd 361.08; found 361.0. HPLC, t_R = 6.36 min, 98.04% purity.

2-(*N*-(3,6-Dimethylbenzo[*d*]isoxazol-5-yl)sulfamoyl)benzoic acid (5n). To a solution of **5m** (70 mg, 0.19 mmol) in MeOH (5 mL) was added 2 M NaOH solution (10 mL). The mixture was stirred at room temperature for 5 h. Upon completion of the reaction, the MeOH was evaporated. The mixture was cooled to 0 °C and acidified to pH 5−6. The precipitated solid was collected by filtration, washed with water and dried to give the title compound as a white solid (53 mg, 79% yield). ^{1}H NMR (400 MHz, DMSO-d_6) δ 13.66 (brs, 1H), 9.21 (s, 1H), 7.75 – 7.68 (m, 2H), 7.65 – 7.60 (m, 1H), 7.60 – 7.54 (m, 1H), 7.48 (s, 1H), 7.46 (s, 1H), 2.45 (s, 3H), 2.12 (s, 3H). ^{13}C NMR (126 MHz, DMSO-d_6) δ 168.8, 160.6, 155.0, 138.3, 137.4, 133.1, 133.0, 131.0, 130.5, 129.2, 128.6, 120.3, 119.6, 110.4, 18.5, 9.4. MS (ESI) *m/z* $[M + H]^+$ calcd 347.06; found 347.0. HPLC, t_R = 2.87 min, 98.71% purity.

2,3-Dichloro-*N*-(3,6-dimethylbenzo[*d*]isoxazol-5-yl)benzenesulfonamide (5o). Compound **5o** was prepared from **13a** and 2,3-dichlorobenzenesulfonyl chloride according to general procedure of step 6 as described for **5a**. White solid, 44% yield. ^{1}H NMR (400 MHz, DMSO-d_6) δ 10.27 (s, 1H), 7.95 (d, J = 8.0 Hz, 1H), 7.80 (d, J = 7.8 Hz, 1H), 7.53 (s, 1H), 7.47 (t, J = 8.0 Hz, 1H),

7.39 (s, 1H), 2.43 (s, 3H), 2.23 (s, 3H). ^{13}C NMR (126 MHz, DMSO-d_6) δ 160.8, 155.0, 140.2, 139.1, 134.7, 134.3, 130.4, 129.6, 129.0, 128.6, 120.6, 120.4, 110.6, 18.5, 9.4. MS (ESI) *m/z* [M + H]$^+$ calcd 370.99; found 371.0. HPLC, t_R = 7.93 min, 98.89% purity.

2,5-Dichloro-*N*-(3,6-dimethylbenzo[*d*]isoxazol-5-yl)benzenesulfonamide (5p). Compound **5p** was prepared from **13a** and 2,5-dichlorobenzenesulfonyl chloride according to general procedure of step 6 as described for **5a**. White solid, 26% yield. ^{1}H NMR (400 MHz, DMSO-d_6) δ 10.28 (s, 1H), 7.80 – 7.74 (m, 3H), 7.55 (s, 1H), 7.40 (s, 1H), 2.45 (s, 3H), 2.23 (s, 3H). ^{13}C NMR (126 MHz, DMSO-d_6) δ 160.8, 155.0, 139.6, 139.1, 134.1, 133.8, 132.1, 130.3, 129.9, 129.7, 120.7, 120.4, 110.6, 18.5, 9.4. MS (ESI) *m/z* [M + H]$^+$ calcd 370.99; found 371.0. HPLC, t_R = 8.63 min, 98.51% purity.

2,6-Dichloro-*N*-(3,6-dimethylbenzo[*d*]isoxazol-5-yl)benzenesulfonamide (5q). Compound **5q** was prepared from **13a** and 2,6-dichlorobenzenesulfonyl chloride according to general procedure of step 6 as described for **5a**. White solid, 65% yield. ^{1}H NMR (400 MHz, DMSO-d_6) δ 10.28 (s, 1H), 7.64 (d, J = 7.6 Hz, 2H), 7.58 (t, J = 6.7 Hz, 1H), 7.55 (s, 1H), 7.39 (s, 1H), 2.43 (s, 3H), 2.26 (s, 3H). ^{13}C NMR (126 MHz, DMSO-d_6) δ 160.8, 154.9, 139.0, 135.6, 134.2 (2 × C), 133.8, 131.8 (2 × C), 130.3, 120.3, 120.1, 110.6, 18.5, 9.4. MS (ESI) *m/z* [M + H]$^+$ calcd 370.99; found 371.0. HPLC, t_R = 6.59 min, 99.67% purity.

***N*-(3,6-Dimethylbenzo[*d*]isoxazol-5-yl)-2-methoxybenzenesulfonamide (5r).** Compound **5r** was prepared from **13a** and 2-methoxybenzenesulfonyl chloride according to general procedure of step 6 as described for **5a**. White solid, 35% yield. ^{1}H NMR (400 MHz, $CDCl_3$) δ 7.80 (d, J =

7.3 Hz, 1H), 7.54 (t, *J* = 7.4 Hz, 1H), 7.44 (s, 1H), 7.28 (s, 1H), 7.05 (d, *J* = 8.5 Hz, 1H), 7.00 (t, *J* = 7.4 Hz, 1H), 6.86 (s, 1H), 4.03 (s, 3H), 2.45 (s, 3H), 2.35 (s, 3H). ^{13}C NMR (126 MHz, $CDCl_3$) δ 160.9, 156.2, 154.9, 135.1, 135.1, 131.1, 130.7, 127.4, 121.1, 120.8, 115.8, 112.3, 111.0, 56.4, 18.8, 10.0. MS (ESI) *m/z* $[M - H]^-$ calcd 331.37; found 331.1. HPLC, t_R = 6.80 min, 99.67% purity.

5-Chloro-*N*-(3,6-dimethylbenzo[*d*]isoxazol-5-yl)-2-methoxybenzenesulfonamide (5s). Compound **5s** was prepared from **13a** and 5-chloro-2-methoxybenzenesulfonyl chloride according to general procedure of step 6 as described for **5a**. White solid, 68% yield. ^{1}H NMR (400 MHz, DMSO-d_6) δ 9.77 (s, 1H), 7.68 (dd, *J* = 8.9, 2.5 Hz, 1H), 7.53 (d, *J* = 2.5 Hz, 1H), 7.51 (s, 1H), 7.43 (s, 1H), 7.29 (d, *J* = 8.9 Hz, 1H), 3.83 (s, 3H), 2.45 (s, 3H), 2.22 (s, 3H). ^{13}C NMR (126 MHz, DMSO-d_6) δ 160.5, 155.3, 154.9, 138.6, 134.3, 131.1, 129.7, 128.5, 123.5, 120.2, 119.9, 114.9, 110.3, 56.4, 18.4, 9.4. MS (ESI) *m/z* $[M + H]^+$ calcd 367.04; found 367.0. HPLC, t_R = 8.07 min, 99.58% purity.

5-Bromo-*N*-(3,6-dimethylbenzo[*d*]isoxazol-5-yl)-2-methoxybenzenesulfonamide (5t). Compound **5t** was prepared from **13a** and 5-bromo-2-methoxybenzenesulfonyl chloride according to general procedure of step 6 as described for **5a**. White solid, 66% yield. ^{1}H NMR (400 MHz, DMSO-d_6) δ 9.77 (s, 1H), 7.80 (dd, *J* = 8.9, 2.2 Hz, 1H), 7.64 (d, *J* = 2.2 Hz, 1H), 7.51 (s, 1H), 7.43 (s, 1H), 7.24 (d, *J* = 8.9 Hz, 1H), 3.83 (s, 3H), 2.46 (s, 3H), 2.22 (s, 3H). ^{13}C NMR (126 MHz, $CDCl_3$) δ 161.2, 155.4, 155.1, 137.8, 135.3, 133.2, 130.8, 129.4, 121.3, 116.4, 114.2, 113.1, 111.3, 56.9, 18.9, 10.1. MS (ESI) *m/z* $[M + H]^+$ calcd 410.99 and 412.99; found 411.0 and 413.0. HPLC, t_R = 9.37 min, 99.72% purity.

***N*-(3,6-Dimethylbenzo[*d*]isoxazol-5-yl)-2-methoxy-5-methylbenzenesulfonamide (5u).** Compound **5u** was prepared from **13a** and 2-methoxy-5-methylbenzenesulfonyl chloride according to general procedure of step 6 as described for **5a**. White solid, 32% yield. ^{1}H NMR (400 MHz, $CDCl_3$) δ 7.59 (d, J = 1.7 Hz, 1H), 7.45 (s, 1H), 7.32 (dd, J = 8.4, 1.6 Hz, 1H), 7.28 (s, 1H), 6.95 (d, J = 8.4 Hz, 1H), 6.87 (brs, 1H), 4.00 (s, 3H), 2.46 (s, 3H), 2.35 (s, 3H), 2.26 (s, 3H). ^{13}C NMR (126 MHz, DMSO-d_6) δ 160.4, 154.8, 154.3, 138.4, 135.1, 131.6, 129.5, 129.0, 127.8, 120.2, 119.4, 112.6, 110.2, 55.8, 19.7, 18.4, 9.4. MS (ESI) *m/z* $[M + H]^+$ calcd 347.10; found 347.0. HPLC, t_R = 8.10 min, 99.44% purity.

***N*-(3,6-Dimethylbenzo[*d*]isoxazol-5-yl)-2,5-dimethoxybenzenesulfonamide (5v).** Compound **5v** was prepared from **13a** and 2,5-dimethoxybenzenesulfonyl chloride according to general procedure of step 6 as described for **5a**. White solid, 48% yield. ^{1}H NMR (400 MHz, DMSO-d_6) δ 9.54 (s, 1H), 7.49 (s, 1H), 7.42 (s, 1H), 7.20 – 7.15 (m, 2H), 7.10 (s, 1H), 3.77 (s, 3H), 3.66 (s, 3H), 2.44 (s, 3H), 2.23 (s, 3H). ^{13}C NMR (126 MHz, DMSO-d_6) δ 160.4, 154.8, 152.1, 150.4, 138.5, 131.5, 128.7, 120.2, 119.7, 119.4, 114.5, 114.1, 110.2, 56.2, 55.7, 18.4, 9.4. MS (ESI) *m/z* $[M + H]^+$ calcd 363.09; found 363.0. HPLC, t_R = 7.27 min, 99.26% purity.

5-Bromo-*N*-(6-hydroxy-3-methylbenzo[*d*]isoxazol-5-yl)-2-methoxybenzenesulfonamide (6a).

Step 1: *N*-(2,4-Dimethoxyphenyl)acetamide (**9b**) was prepared from **9a** according to general procedure of step 1 as described for **5a**. Brown solid, 71% yield. ^{1}H NMR (400 MHz, DMSO-d_6) δ 8.99 (brs, 1H), 7.64 (d, J = 8.7 Hz, 1H), 6.59 (s, 1H), 6.45 (d, J = 8.8 Hz, 1H), 3.79 (s, 3H), 3.73 (s, 3H), 2.01 (s, 3H). MS (ESI) *m/z* $[M + H]^+$ calcd 196.09; found 196.1.

Step 2: *N*-(5-Acetyl-4-hydroxy-2-methoxyphenyl)acetamide (**10b**) was prepared from **9b** according to general procedure of step 2 as described for **5a**. Yellow solid, 78% yield. ^{1}H NMR (500 MHz, DMSO-d_6) δ 12.54 (s, 1H), 9.17 (s, 1H), 8.26 (s, 1H), 6.59 (s, 1H), 3.88 (s, 3H), 2.52 (s, 3H), 2.05 (s, 3H). MS (ESI) *m/z* $[M + H]^+$ calcd 224.08; found 224.1.

Step 3: *N*-(4-Hydroxy-5-(1-(hydroxyimino)ethyl)-2-methoxyphenyl)acetamide (**11b**) was prepared from **10b** according to general procedure of step 3 as described for **5a**. Pale red solid, 94% yield. ^{1}H NMR (500 MHz, DMSO-d_6) δ 11.74 (s, 1H), 11.33 (s, 1H), 9.03 (s, 1H), 7.84 (s, 1H), 6.54 (s, 1H), 3.80 (s, 3H), 2.17 (s, 3H), 2.02 (s, 3H). MS (ESI) *m/z* $[M + H]^+$ calcd 239.10; found 239.1.

Step 4: *N*-(6-Methoxy-3-methylbenzo[*d*]isoxazol-5-yl)acetamide (**12b**) was prepared from **11b** according to general procedure of step 4 as described for **5a**. Yellow solid, 70% yield. ^{1}H NMR (500 MHz, DMSO-d_6) δ 9.26 (brs, 1H), 8.24 (s, 1H), 7.36 (s, 1H), 3.94 (s, 3H), 2.47 (s, 3H), 2.11 (s, 3H). MS (ESI) *m/z* $[M + H]^+$ calcd 221.08; found 221.1.

Step 5: 6-Methoxy-3-methylbenzo[*d*]isoxazol-5-amine (**13b**) was prepared from **12b** according to general procedure of step 5 as described for **5a**. Brown solid, 96% yield. ^{1}H NMR (500 MHz, DMSO-d_6) δ 7.14 (s, 1H), 6.80 (s, 1H), 4.80 (brs, 2H), 3.88 (s, 3H), 2.39 (s, 3H). MS (ESI) *m/z* $[M + H]^+$ calcd 179.07; found 179.0.

Step 6: To a solution of compound **13b** (800 mg, 4.5 mmol) in CH_2Cl_2 (15 mL) was added a 1 M BBr_3 solution (1.3 mL, 13.5 mmol) in CH_2Cl_2. The reaction was monitored by TLC. Upon completion, the reaction was quenched with saturated ammonium chloride solution, and then a mixed solvent of ice-water and CH_2Cl_2 was added. The mixture was basified to pH 6−8 with aqueous $NaHCO_3$ solution and stirred for 1 h. The remaining solid was filtered off and the filtrate was separated. The organic layer was washed with brine, dried over Na_2SO_4, and

concentrated under reduced pressure to give 5-amino-3-methylbenzo[*d*]isoxazol-6-ol (**14**) as a brown solid (670 mg, 91% yield). ^{1}H NMR (500 MHz, DMSO-d_6) δ 6.85 (s, 1H), 6.76 (s, 1H), 2.36 (s, 3H). MS (ESI) *m/z* $[M + H]^+$ calcd 165.06; found 165.0.

Step 7: To a solution of **14** (840 mg, 5.12 mmol) in CH_2Cl_2 (15 mL) were added 5-bromo-2-methoxybenzenesulfonyl chloride (1.5 g, 5.12 mmol) and pyridine (1 mL). The mixture was stirred at room temperature for 2 h. The reaction mixture was extracted with CH_2Cl_2 and washed successively with 1 N HCl and brine. The organic layer was dried over Na_2SO_4 and concentrated under reduced pressure. The residue was purified by silica gel chromatography to give the title compound **6a** as a white solid (1.5 g, 71% yield). ^{1}H NMR (500 MHz, DMSO-d_6) δ 10.70 (brs, 1H), 9.09 (brs, 1H), 7.74 (dd, J = 8.8, 2.5 Hz, 1H), 7.69 (d, J = 2.5 Hz, 1H), 7.54 (s, 1H), 7.18 (d, J = 8.9 Hz, 1H), 6.88 (s, 1H), 3.82 (s, 3H), 2.44 (s, 3H). ^{13}C NMR (126 MHz, DMSO-d_6) δ 161.1, 156.2, 154.7, 154.0, 137.0, 131.1, 129.7, 122.3, 117.8, 115.2, 113.6, 110.4, 94.4, 56.5, 9.3. MS (ESI) *m/z* $[M + H]^+$ calcd 412.97 and 414.97; found 412.9 and 414.9. HPLC, t_R = 6.39 min, 98.84% purity.

Ethyl-2-((5-((5-bromo-2-methoxyphenyl)sulfonamido)-3-methylbenzo[*d*]isoxazol-6-yl)oxy)acetate (6b). To a solution of **6a** (200 mg, 0.48 mmol) in acetone (10 mL) was added ethyl chloracetate (71.1 mg, 0.58 mmol), followed by K_2CO_3 (199.0 mg, 1.44 mmol) and KI (8.0 mg, 0.048 mmol). The mixture was stirred at 50 ℃. The solvent was removed in vacuo. The residue was extracted with EtOAc. The organic layer was washed with brine, dried over Na_2SO_4, and concentrated under reduced pressure. The crude product was purified by silica gel chromatography to give the title compound as a white solid (80 mg, 33% yield). ^{1}H NMR (500 MHz, DMSO-d_6) δ 9.18 (s, 1H), 7.73 (dd, J = 8.8, 2.6 Hz, 1H), 7.69 (d, J = 2.5 Hz, 1H), 7.67 (s,

1H), 7.27 (s, 1H), 7.16 (d, J = 8.9 Hz, 1H), 4.75 (s, 2H), 4.11 (q, J = 7.1 Hz, 2H), 3.82 (s, 3H), 2.48 (s, 3H), 1.17 (t, J = 7.1 Hz, 3H). ^{13}C NMR (126 MHz, DMSO-d_6) δ 167.7, 160.8, 155.9, 154.9, 153.7, 137.0, 131.1, 129.5, 123.3, 117.5, 115.5, 114.9, 110.6, 94.1, 65.8, 60.9, 56.4, 13.9, 9.4. MS (ESI) *m/z* $[M + H]^+$ calcd 499.01 and 501.01; found 499.0 and 501.01. HPLC, t_R = 8.46 min, 99.27% purity.

2-((5-((5-Bromo-2-methoxyphenyl)sulfonamido)-3-methylbenzo[*d*]isoxazol-6-yl)oxy)acetic acid (6c). Compound **6c** was prepared from **6b** according to general procedure as described for **5n**. White solid, 76% yield. ^{1}H NMR (400 MHz, DMSO-d_6) δ 13.10 (brs, 1H), 9.15 (brs, 1H), 7.73 (dd, J = 8.8, 2.6 Hz, 1H), 7.70 (d, J = 2.5 Hz, 1H), 7.66 (s, 1H), 7.26 (s, 1H), 7.15 (d, J = 8.8 Hz, 1H), 4.68 (s, 2H), 3.82 (s, 3H), 2.48 (s, 3H). ^{13}C NMR (126 MHz, DMSO-d_6) δ 169.2, 160.7, 155.9, 154.9, 153.5, 137.2, 131.1, 129.2, 123.5, 116.7, 115.1, 114.9, 110.6, 94.2, 66.1, 56.4, 9.4. MS (ESI) *m/z* $[M - H]^-$ calcd 468.98 and 470.98; found 468.9 and 470.9. HPLC, t_R = 3.02 min, 97.11% purity.

2-((5-((5-Bromo-2-methoxyphenyl)sulfonamido)-3-methylbenzo[*d*]isoxazol-6-yl)oxy)-*N*-ethylacetamide (6d). To a solution of the acid **6c** (80.0 mg, 0.17 mmol) in DMF (8 mL) were added DIPEA (87.9 mg, 0.68 mmol) and HATU (98.8 mg, 0.26 mmol). The reaction mixture was stirred for 15 min. 2.0 M ethanamine solution in THF (0.13 mL, 0.26 mmol) and DMAP (8mg, 10%) was then added to the mixture. After 12 h, the mixture was diluted with water, extracted with EtOAc, and washed successively with 1 N HCl and brine. The organic layer was dried over Na_2SO_4 and concentrated in vacuo. The crude product was purified by silica gel chromatography to give the title compound as a white solid (40 mg, 47% yield). ^{1}H NMR (400

MHz, CDCl3) δ 7.95 (d, *J* = 2.4 Hz, 1H), 7.64 (dd, *J* = 8.8, 2.4 Hz, 1H), 7.55 (s, 1H), 7.38 (s, 1H), 6.94 (d, *J* = 8.4 Hz, 1H), 6.94 (s, 1H), 6.64 (brs, 1H),4.53 (s, 2H), 3.97 (s, 3H), 3.41 – 3.31 (m, 2H), 2.50 (s, 3H), 1.14 (t, *J* = 7.3 Hz, 3H). ^{13}C NMR (126 MHz, DMSO-d_6) δ 166.0, 161.2, 155.9, 155.0, 153.4, 137.1, 131.3, 129.7, 123.3, 118.6, 115.0, 114.8, 110.6, 93.5, 67.7, 56.1, 33.1, 14.7, 9.4. MS (ESI) *m/z* [M + H]+ calcd 498.03 & 500.02; found 498.0 & 499.9. HPLC, t_R = 6.46 min, 96.01% purity.

***N*-(2-Acetamidoethyl)-2-((5-((5-bromo-2-methoxyphenyl)sulfonamido)-3-methylbenzo[*d*]isoxazol-6-yl)oxy)acetamide (6e).** Compound **6e** was prepared from **6c** and *N*-(2-aminoethyl)acetamide according to general procedure as described for **6d**. White solid, 48% yield. ^{1}H NMR (400 MHz, $CDCl_3$) δ 8.69 (s, 1H), 8.20 (brs, 1H), 8.00 (d, *J* = 2.4 Hz, 1H), 7.73 (s, 1H), 7.56 (dd, *J* = 8.8, 2.4 Hz, 1H), 6.89 (s, 1H), 6.80 (d, *J* = 8.8 Hz, 1H), 6.19 (brs, 1H), 4.34 (s, 2H), 3.61 (s, 3H), 3.42 (t, *J* = 5.6 Hz, 4H), 2.54 (s, 3H), 2.07 (s, 3H). ^{13}C NMR (126 MHz, $CDCl_3$) δ 173.7, 167.1, 161.8, 156.1, 155.4, 153.1, 137.4, 133.1, 130.3, 123.4, 119.0, 116.2, 114.1, 112.4, 92.7, 67.6, 56.5, 41.8, 39.8, 23.1, 10.1. MS (ESI) *m/z* $[M + H]^+$ calcd 555.05 and 557.05; found 554.8 and 556.9. HPLC, t_R = 5.62 min, 98.76% purity.

2-((5-((5-Bromo-2-methoxyphenyl)sulfonamido)-3-methylbenzo[*d*]isoxazol-6-yl)oxy)-*N*-(2-morpholinoethyl)acetamide (6f). Compound **6f** was prepared from **6c** and 2-morpholinoethan-1-amine according to general procedure as described for **6d**. White solid, 32% yield. ^{1}H NMR (400 MHz, $CDCl_3$) δ 7.99 (d, *J* = 2.4 Hz, 1H), 7.61 (dd, *J* = 8.8, 2.4 Hz, 1H), 7.61 (s, 1H), 7.09 (brs, 1H), 6.94 (s, 1H), 6.90 (d, *J* = 8.8 Hz, 1H), 4.55 (s, 2H), 3.91 (s, 3H), 3.68 – 3.55 (m, 4H), 3.45 (q, *J* = 5.5 Hz, 2H), 2.53 (t, *J* = 6.0 Hz, 2H), 2.51 (s, 3H), 2.49 – 2.41 (m, 4H). ^{13}C NMR

(126 MHz, DMSO-d_6) δ 166.4, 161.1, 155.9, 155.0, 153.4, 137.2, 131.2, 129.6, 123.2, 118.5, 115.1, 114.8, 110.6, 93.5, 67.7, 66.0 (2 ×C), 57.3, 56.2, 53.2 (2 ×C), 35.7, 9.4. MS (ESI) *m/z* [M + H]$^+$ calcd 583.08 & 585.08; found 583.0 & 585.0. HPLC, t_R = 6.78 min, 97.02% purity.

5-Bromo-2-methoxy-*N*-(3-methyl-6-propoxybenzo[*d*]isoxazol-5-yl)benzenesulfonamide (6g). Compound **6g** was prepared from **6a** and iodoethane according to general procedure as described for **6b**. White solid, 32% yield. ^{1}H NMR (500 MHz, DMSO-d_6) δ 9.26 (s, 1H), 7.75 (dd, *J* = 8.7, 2.6 Hz, 1H), 7.73 (d, *J* = 2.5 Hz, 1H), 7.61 (s, 1H), 7.25 (s, 1H), 7.16 (d, *J* = 8.8 Hz, 1H), 3.84 (t, *J* = 6.6 Hz, 2H), 3.68 (s, 3H), 2.48 (s, 3H), 1.54 – 1.45 (m, 2H), 0.82 (t, *J* = 7.4 Hz, 3H). ^{13}C NMR (126 MHz, DMSO-d_6) δ 161.6, 155.9, 155.2, 154.8, 136.8, 130.9, 130.4, 123.1, 118.4, 115.2, 113.8, 110.6, 92.6, 70.3, 56.2, 21.3, 10.1, 9.4. MS (ESI) *m/z* [M + H]$^+$ calcd 455.02 & 457.02; found 455.0 & 457.0. HPLC, t_R = 10.73 min, 96.75% purity.

5-Bromo-*N*-(6-ethoxy-3-methylbenzo[*d*]isoxazol-5-yl)-2-methoxybenzenesulfonamide (6h). Compound **6h** was prepared from **6a** and 1-iodopropane according to general procedure as described for **6b**. White solid, 31% yield. ^{1}H NMR (500 MHz, DMSO-d_6) δ 9.25 (s, 1H), 7.76 (dd, *J* = 8.9, 2.6 Hz, 1H), 7.70 (d, *J* = 2.5 Hz, 1H), 7.63 (s, 1H), 7.24 (s, 1H), 7.18 (d, *J* = 8.9 Hz, 1H), 3.94 (q, *J* = 7.0 Hz, 2H), 3.74 (s, 3H), 2.48 (s, 3H), 1.09 (t, *J* = 7.0 Hz, 3H). ^{13}C NMR (126 MHz, $CDCl_3$) δ 161.0, 155.8, 155.3, 151.6, 137.6, 133.3, 128.7, 123.6, 115.1, 114.1, 112.7, 112.2, 92.6, 65.2, 56.7, 14.7, 10.1. MS (ESI) *m/z* [M + H]$^+$ calcd 441.00 & 443.00; found 441.0 & 443.0. HPLC, t_R = 9.13 min, 95.08% purity.

5-Bromo-2-methoxy-*N*-(6-methoxy-3-methylbenzo[*d*]isoxazol-5-yl)benzenesulfonamide (6i). Compound **6i** was prepared from **13b** and 5-bromo-2-methoxybenzenesulfonyl chloride according to general procedure of step 7 as described for **6a**. White solid, 84% yield. ^{1}H NMR (500 MHz, DMSO-d_6) δ 9.31 (s, 1H), 7.75 (dd, J = 8.8, 2.5 Hz, 1H), 7.64 (d, J = 2.5 Hz, 1H), 7.62 (s, 1H), 7.24 (s, 1H), 7.20 (d, J = 8.9 Hz, 1H), 3.84 (s, 3H), 3.63 (s, 3H), 2.48 (s, 3H). ^{13}C NMR (126 MHz, $CDCl_3$) δ 161.1, 155.7, 155.3, 152.6, 137.7, 133.3, 128.6, 123.5, 115.4, 113.8, 113.0, 112.6, 92.0, 56.6, 56.5, 10.1. MS (ESI) *m/z* $[M + H]^+$ calcd 426.99 and 428.99; found 426.9 and 428.9. HPLC, t_R = 7.12 min, 99.43% purity.

5-Bromo-2-methoxy-*N*-(3-methyl-6-(methylamino)benzo[*d*]isoxazol-5-yl)benzenesulfonamide (6j).

Step 1: 3-Fluorophenol **15** (10 g, 89.2 mmol) was dissolved in acetic anhydride (8.5 mL). Upon addition of 3-5 drops of concentrated H_2SO_4, the temperature rose to about 80 °C. After being cooled to room temperature, the mixture was poured into a solution of 1 g $NaHCO_3$ dissolved in 100 mL of cold water and extracted with EtOAc. The organic layer was washed with saturated $NaHCO_3$ solution, dried over Na_2SO_4, and evaporated in vacuo to give the essentially pure product 3-fluorophenyl acetate (**16**) as a colorless oil (10.5 g, 76% yield). ^{1}H NMR (400 MHz, $CDCl_3$) δ 7.33 (td, J = 8.2, 6.6 Hz, 1H), 6.95 (td, J = 8.4, 2.4 Hz, 1H), 6.90 (dd, J = 8.1, 1.6 Hz, 1H), 6.86 (dt, J = 9.6, 2.4 Hz, 1H), 2.30 (s, 3H).

Step 2: Compound **16** (10.5 g, 68.1 mmol) was cooled with an ice-bath, treated portionwise with aluminum chloride (12.7 g, 95.3 mmol). The reaction was stirred at 190 °C for 1 h, and cooled to obtain a solid. A mixture of ice-water, hydrochloric acid and CH_2Cl_2 was added to the solid. The resultant mixture was stirred for several minutes. The organic layer was washed sequentially

with water, saturated $NaHCO_3$ and brine, dried over Na_2SO_4, and concentrated in vacuo to obtain the product 4-fluoro-2-hydroxyacetophenone (**17**) as a yellow oil (7.5 g, 71% yield). ^{1}H NMR (400 MHz, $CDCl_3$) δ 12.57 (d, *J* = 1.4 Hz, 1H), 7.74 (dd, *J* = 8.8, 6.4 Hz, 1H), 6.65 (dd, *J* = 10.3, 2.3 Hz, 1H), 6.61 (td, *J* = 8.4, 2.4 Hz, 1H), 2.60 (s, 3H).

Step 3: A mixture of compound **17** (6.2 g, 40.0 mmol), hydroxylamine hydrochloride (5.6 g, 80.0 mmol), and sodium acetate (4.9 g, 60.0 mmol) were dissolved in a mixed solvent of EtOH-H_2O (7:3, 80 mL). The mixture was heated under reflux for 70 min. Upon completion of the reaction, water (50 mL) was added to the mixture. The precipitated solid was filtered, washed with water and dried to give 1-(4-fluoro-2-hydroxyphenyl)ethan-1-one oxime (**18**) as a white solid (5.8 g, 86% yield). ^{1}H NMR (400 MHz, $CDCl_3$) δ 11.48 (s, 1H), 7.39 (dd, *J* = 8.8, 6.4 Hz, 1H), 7.21 (brs, 1H), 6.67 (dd, *J* = 10.4, 2.6 Hz, 1H), 6.62 (td, *J* = 8.4, 2.4 Hz, 1H), 2.34 (s, 3H).

Step 4: To a solution of compound **18** (5.8 g, 34.3 mmol) in DMF (70 mL) were added NaOAc (6.4 g, 77.5 mmol) and acetic anhydride (7.5 mL, 79.8 mmol). The mixture was heated at reflux for 4 h. The mixture was allowed to cool, poured into water and extracted with EtOAc. The organic layer was washed with brine, dried over Na_2SO_4, and concentrated in vacuo. The residue was purified by silica gel chromatography to give 6-fluoro-3-methylbenzo[*d*]isoxazole (**19**) as a white solid (4.7 g, 90% yield). ^{1}H NMR (400 MHz, $CDCl_3$) δ 7.57 (dd, *J* = 8.6, 5.1 Hz, 1H), 7.23 (dd, *J* = 8.5, 1.8 Hz, 1H), 7.07 (td, *J* = 8.9, 2.1 Hz, 1H), 2.56 (s, 3H).

Step 5: To an ice-cold solution of compound **19** (3.0 g, 19.8 mmol) in concentrated H_2SO_4 (21 mL) was added dropwise with nitric acid (1.7 mL). The reaction mixture temperature was kept below 15 °C. The mixture was stirred for 1 h on ice-bath and then allowed to warm to room temperature and stirred for 3 h. Upon completion of the reaction, the mixture was poured onto ice. The precipitated solid was filtered and dried to give 6-fluoro-3-methyl-5-

nitrobenzo[*d*]isoxazole (**20**) as a white solid (3.2 g, 82% yield). ^{1}H NMR (400 MHz, $CDCl_3$) δ 8.45 (d, *J* = 6.9 Hz, 1H), 7.45 (d, *J* = 10.0 Hz, 1H), 2.65 (s, 3H).

Step 6: To a solution of **20** (1.0 g, 5.1 mmol) in a mixed solvent of EtOH-THF (2:1, 30 mL) was added methylamine solution 33 wt.% in methanol (2.64 mL, 17.8 mmol). The mixture was heated at 45 °C with stirring in a sealed reaction vessel for 3 h. The slurry was filtered and the cake was dried to give *N*, 3-dimethyl-5-nitrobenzo[*d*]isoxazol-6-amine (**21**) as a bright orange solid (1.0 g, 95% yield). ^{1}H NMR (400 MHz, DMSO-d_6) δ 8.66 (s, 1H), 8.19 (q, *J* = 4.2 Hz, 1H), 6.94 (s, 1H), 2.97 (d, *J* = 4.9 Hz, 3H), 2.50 (s, 3H).

Step 7: To the compound **21** (250 mg, 1.2 mmol) in AcOH (4 mL) at 40 °C was added a solution of $SnCl_2 \cdot 2H_2O$ (812.3 mg, 3.6 mmol) in concentrated HCl (2 mL). The reaction mixture was heated at 40 °C for 0.5 h. The reaction mixture was allowed to cool and adjusted to pH 7-9 with aqueous NaOH. The mixture was extracted with EtOAc (3 × 100 mL). The organic layer was washed with saturated $NaHCO_3$ solution and brine, dried over Na_2SO_4, and concentrated under reduced pressure. The residue was purified by silica gel chromatograph to give N^6, 3-dimethylbenzo[*d*]isoxazole-5,6-diamine (**22**) as a light yellow solid (83 mg, 39% yield). ^{1}H NMR (400 MHz, DMSO-d_6) δ 6.71 (s, 1H), 6.46 (s, 1H), 5.45 (q, *J* = 4.4 Hz, 1H), 4.54 (brs, 2H), 2.78 (d, *J* = 4.8 Hz, 3H), 2.33 (s, 3H). MS (ESI) *m/z* $[M + H]^+$ calcd 178.09; found 178.1.

Step 8: The title compound **6j** was prepared from **22** and 5-bromo-2-methoxybenzenesulfonyl chloride according to general procedure of step 7 as described for **6a**. White solid, 71% yield. ^{1}H NMR (400 MHz, DMSO-d_6) δ 9.51 (brs, 1H), 7.81 (dd, *J* = 8.9, 2.5 Hz, 1H), 7.62 (d, *J* = 2.5 Hz, 1H), 7.26 (d, *J* = 8.9 Hz, 1H), 7.00 (s, 1H), 6.55 (s, 1H), 5.69 (brs, 1H), 3.93 (s, 3H), 2.72 (s, 3H), 2.29 (s, 3H). ^{13}C NMR (126 MHz, $CDCl_3$) δ 164.6, 155.4, 154.5, 149.4, 137.9, 133.5, 128.8,

119.7, 118.5, 114.3, 113.5, 111.7, 89.5, 57.3, 30.5, 9.8. MS (ESI) *m/z* $[M + H]^+$ calcd 426.00 and 428.00; found 425.9 and 427.9. HPLC, t_R = 6.79 min, 96.51% purity.

2-Chloro-*N*-(6-methoxy-3-methylbenzo[*d*]isoxazol-5-yl)benzenesulfonamide (6k). Compound **6k** was prepared from **13b** and 2-chlorobenzenesulfonyl chloride according to general procedure of step 7 as described for **6a**. White solid, 78% yield. ^{1}H NMR (500 MHz, DMSO-d_6) δ 9.75 (s, 1H), 7.74 (dd, *J* = 7.9, 1.5 Hz, 1H), 7.67 (dd, *J* = 8.0, 1.1 Hz, 1H), 7.62 (s, 1H), 7.61 (td, *J* = 7.8, 1.2 Hz, 1H), 7.39 (td, *J* = 7.8, 1.2 Hz, 1H), 7.20 (s, 1H), 3.49 (s, 3H), 2.47 (s, 3H). ^{13}C NMR (126 MHz, DMSO-d_6) δ 161.9, 156.6, 154.9, 137.9, 134.0, 131.5, 131.3, 130.6, 127.1, 122.2, 120.2, 114.2, 92.3, 55.9, 9.4. MS (ESI) *m/z* $[M + H]^+$ calcd 353.03; found 353.0. HPLC, t_R = 6.40 min, 99.75% purity.

2,5-Dichloro-*N*-(6-methoxy-3-methylbenzo[*d*]isoxazol-5-yl)benzenesulfonamide (6l). Compound **6l** was prepared from **13b** and 2,5-dichlorobenzenesulfonyl chloride according to general procedure of step 7 as described for **6a**. White solid, 54% yield. ^{1}H NMR (500 MHz, DMSO-d_6) δ 10.07 (s, 1H), 7.76 – 7.70 (m, 3H), 7.67 (s, 1H), 7.25 (s, 1H), 3.52 (s, 3H), 2.49 (s, 3H). ^{13}C NMR (126 MHz, DMSO-d_6) δ 162.1, 156.8, 155.0, 139.8, 133.6, 133.3, 131.5, 130.2, 129.5, 121.7, 121.1, 114.3, 92.5, 55.9, 9.4. MS (ESI) *m/z* $[M + H]^+$ calcd 386.99; found 387.0. HPLC, t_R = 7.68 min, 99.68% purity.

5-Chloro-2-methoxy-*N*-(6-methoxy-3-methylbenzo[*d*]isoxazol-5-yl)benzenesulfonamide (6m). Compound **6m** was prepared from **13b** and 5-chloro-2-methoxybenzenesulfonyl chloride according to general procedure of step 7 as described for **6a**. White solid, 66% yield. ^{1}H NMR

(500 MHz, DMSO-d_6) δ 9.32 (s, 1H), 7.65(dd, J = 8.5, 2.5 Hz, 1H), 7.63 (s, 1H), 7.52 (d, J = 2.7 Hz, 1H), 7.25 (d, J = 9.7 Hz, 1H), 7.24 (s, 1H), 3.85 (s, 3H), 3.62 (s, 3H), 2.48 (s, 3H). ^{13}C NMR (126 MHz, DMSO-d_6) δ 161.5, 155.9, 155.6, 154.9, 134.1, 129.4, 128.3, 123.1, 122.8, 118.7, 114.6, 114.1, 92.3, 56.5, 56.3, 9.4. MS (ESI) m/z $[M + H]^+$ calcd 383.04; found 383.0. HPLC, t_R = 7.74 min, 99.00% purity.

2-Methoxy-*N*-(6-methoxy-3-methylbenzo[*d*]isoxazol-5-yl)-5-methylbenzenesulfonamide (6n). Compound **6n** was prepared from **13b** and 2-methoxy-5-methylbenzenesulfonyl chloride according to general procedure of step 7 as described for **6a**. White solid, 54% yield. ^{1}H NMR (500 MHz, DMSO-d_6) δ 8.86 (s, 1H), 7.60 (s, 1H), 7.42 (s, 1H), 7.36 (d, J = 8.4 Hz, 1H), 7.24 (s, 1H), 7.08 (d, J = 8.4 Hz, 1H), 3.83 (s, 3H), 3.67 (s, 3H), 2.46 (s, 3H), 2.19 (s, 3H). ^{13}C NMR (126 MHz, DMSO-d_6) δ 161.1, 155.0, 154.8, 154.5, 135.0, 129.3, 128.7, 127.0, 123.5, 116.4, 114.0, 112.4, 92.3, 56.4, 56.0, 19.7, 9.4. MS (ESI) m/z $[M + H]^+$ calcd 363.09; found 363.0. HPLC, t_R = 5.57 min, 98.89% purity.

3-Methyl-5-(6-morpholino-1-propyl-1*H*-benzo[*d*]imidazol-2-yl)benzo[*d*]isoxazole (7a).

Step 1: Methyl 4-acetoxybenzoate (**23**) (11g, 56.7 mmol), $AlCl_3$ (22.7 g, 170.1 mmol), and KCl (4.4 g, 59.5 mmol) were mixed in a 500 mL three-necked round-bottom flask, which was equipped with water condenser and gas absorber. The mixture was heated at 120 ℃ for 30 min, and then heated at 170 ℃ for 1 h. After cooling, a mixed solvent of 2 N HCl (200 mL) and EtOH (40 mL) was added to the reaction mixture. The resulting suspension was refluxed for 0.5 h. The crude product was filtered using Büchner funnel and recrystallized with EtOH to give 3-acetyl-4-hydroxybenzoic acid (**24**) as a yellow solid (9.0 g, 88% yield). ^{1}H NMR (500 MHz, DMSO-d_6) δ

12.23 (s, 1H), 8.37 (d, J = 2.1 Hz, 1H), 8.03 (dd, J = 8.7, 2.2 Hz, 1H), 7.06 (d, J = 8.7 Hz, 1H), 2.67 (s, 3H). MS (ESI) *m/z* $[M - H]^-$ calcd 179.16; found 179.1.

Step 2: To a stirred solution of **24** (9.0 g, 50.0 mmol) in 100 mL of MeOH, under ice-cooling, was added dropwise with thionyl chloride (8.9 g, 75.0 mmol). The reaction mixture was stirred for 3 h at 65 ℃. The solvent was distilled out and water was added. The crude product was filtered, washed with saturated $NaHCO_3$ and dried to give methyl 3-acetyl-4-hydroxybenzoate (**25a**) as a pale-yellow solid (6 g, 62% yield). ^{1}H NMR (500 MHz, $CDCl_3$) δ 12.68 (s, 1H), 8.49 (d, J = 1.9 Hz, 1H), 8.14 (dd, J = 8.8, 1.9 Hz, 1H), 7.02 (d, J = 8.8 Hz, 1H), 3.93 (s, 3H), 2.71 (s, 3H).

Step 3: To a mixed solvent of EtOH-H_2O (7:3, 100 mL) were added compound **25a** (6.4 g, 33.0 mmol), hydroxylamine hydrochloride (3.7 g, 52.8 mmol) and NaOAc (4.3 g, 52.8 mmol). The mixture was heated under reflux for 70 min. The reaction mixture was cooled and concentrated under reduced pressure to allow precipitation of a solid. Water (50 mL) was added and the precipitated solid was filtered, washed and dried to give methyl-4-hydroxy-3-(1-(hydroxyimino)ethyl)benzoate (**26a**) as a white solid (6.4 g, 92% yield). ^{1}H NMR (500 MHz, DMSO-d_6) δ 12.19 (s, 1H), 11.72 (s, 1H), 8.03 (d, J = 2.0 Hz, 1H), 7.84 (dd, J = 8.6, 2.0 Hz, 1H), 6.98 (d, J = 8.6 Hz, 1H), 3.82 (s, 3H), 2.28 (s, 3H).

Step 4: To a solution of compound **26a** (5.4 g, 25.8 mmol) in 1,4-dioxane (30 mL) was added DMF-DMA (15.7 mL) with vigorous stirring. The mixture was stirred with heating at 100 °C for 7 min. The reaction mixture was cooled and concentrated under reduced pressure. Water (40 mL) was added and the precipitated solid was filtered. The obtained solid was dried and recrystallized (EA : PE = 1:2) to give methyl 3-methylbenzo[*d*]isoxazole-5-carboxylate (**27a**) as a white solid

(3.0 g, 61% yield). ^{1}H NMR (500 MHz, $CDCl_3$) δ 8.39 (s, 1H), 8.25 (d, *J* = 8.7 Hz, 1H), 7.57 (d, *J* = 8.8 Hz, 1H), 3.97 (s, 3H), 2.63 (s, 3H). MS (ESI) *m/z* $[M + H]^-$ calcd 192.19; found 192.1.

Step 5: To a solution of **27a** (3.0 g, 15.7 mmol) in MeOH (30 mL) was added 2 M aqueous NaOH (78.5 mL), the reaction was stirred at room temperature. After 5 h, the MeOH was evaporated. The mixture was cooled to 0 °C and acidified to pH 5−6. The precipitated solid was collected by filtration, washed with water and dried to give 3-methylbenzo[*d*]isoxazole-5-carboxylic acid (**28a**) as a white solid (2.7 g, 97% yield). ^{1}H NMR (400 MHz, DMSO-d_6) δ 13.18 (s, 1H), 8.47 (d, *J* = 1.0 Hz, 1H), 8.19 (dd, *J* = 8.8, 1.6 Hz, 1H), 7.78 (d, *J* = 8.8 Hz, 1H), 2.61 (s, 3H).

Step 6: To a solution of 2-chloro-4-fluoro-1-nitrobenzene (**29**) (3.0 g, 17.1 mmol) in DMF (10 mL) were added morpholine (1.6 g, 17.9 mmol) and K_2CO_3 (3.6 g, 25.7 mmol). The reaction mixture was stirred at 100 °C for 1 h and then added water (50 mL). The precipitated solid was filtered, washed with water, and dried to give 4-(3-chloro-4-nitrophenyl)morpholine (**30a**) as a yellow solid (4.0 g, 97% yield). ^{1}H NMR (400 MHz, DMSO-d_6) δ 8.03 (d, *J* = 9.4 Hz, 1H), 7.11 (d, *J* = 2.6 Hz, 1H), 7.00 (dd, *J* = 9.4, 2.6 Hz, 1H), 3.71 (t, *J* = 4.8 Hz, 4H), 3.41 (t, *J* = 4.8 Hz, 4H).

Step 7: To a solution of compound **30a** (500 mg, 2.07 mmol) in DMSO (5 mL) were added propan-1-amine (367.1 mg, 6.21 mmol) and DIPEA (0.5 mL, 3.11 mmol). The reaction mixture was stirred overnight at 95 °C. Water (15 mL) was added with stirring for 10 min. The precipitated solid was filtered, washed and dried to give 5-morpholino-2-nitro-*N*-propylaniline (**31a**) as a yellow solid (500 mg, 91% yield). ^{1}H NMR (500 MHz, $CDCl_3$) δ 8.39 (brs, 1H), 8.08 (d, *J* = 9.7 Hz, 1H), 6.22 (dd, *J* = 9.7, 2.6 Hz, 1H), 5.89 (d, *J* = 2.5 Hz, 1H), 3.85 (t, *J* = 5.0 Hz, 4H), 3.36 (t, *J* = 5.0 Hz, 4H), 3.24 – 3.20 (m, 2H), 1.82 – 1.74 (m, 2H), 1.06 (t, *J* = 7.4 Hz, 3H).

Step 8: A mixture of **31a** (500 mg, 1.88 mmol), 10% Pd on carbon (wetted with ca. 55% water) (80 mg), was dissolved in MeOH–THF (2:3, 25 mL), which was stirred under H_2 atmosphere overnight. The mixture was filtered using Celite, and the filtrate was concentrated to give the crude product 5-morpholino-N^1-propylbenzene-1,2-diamine (**32a**) as a purple oil (371 mg, 84% yield). The crude product was used without further purification.

Step 9: To a solution of compound **28a** (200 mg, 1.13 mmol) in DMF (10 mL) were added DIPEA (438.2 mg, 3.39 mmol) and HATU (646.4 mg, 1.70 mmol). The reaction mixture was stirred for 15 min. Compound **32a** (320.0 mg, 1.36 mmol) was then added to the mixture. After 12 h, the reaction mixture was diluted with water and extracted with EtOAc (3 × 20 mL). The combined organic layer was dried over Na_2SO_4 and concentrated under reduced pressure. The crude product was purified by silica gel chromatography to afford 3-methyl-*N*-(4-morpholino-2-(propylamino)phenyl)benzo[*d*]isoxazole-5-carboxamide (**33a**) as a white solid (230 mg, 52% yield). ^{1}H NMR (500 MHz, DMSO-d_6) δ 9.64 (s, 1H), 8.53 (s, 1H), 8.24 (d, J = 8.0 Hz, 1H), 7.80 (d, J = 8.7 Hz, 1H), 6.97 (d, J = 8.9 Hz, 1H), 6.23 – 6.21 (m, 2H), 4.85 (t, J = 5.2 Hz, 1H), 3.74 (t, J = 4.0 Hz, 4H), 3.08 (t, J = 4.0 Hz, 4H), 3.06 – 3.02 (m, 2H), 2.62 (s, 3H), 1.60 – 1.52 (m, 2H), 0.92 (t, J = 7.4 Hz, 3H).

Step 10: Compound **33a** (200 mg, 0.51 mmol) was dissolved in acetic acid (5 mL) and the mixture was stirred at 120 °C for 4 h. The reaction mixture was then neutralized with aqueous $NaHCO_3$ and extracted with EtOAc. The organic layer was separated, dried over Na_2SO_4 and concentrated under reduced pressure. The crude product was purified by silica gel chromatography to afford the title compound (**7a**) as a white solid (61 mg, 32% yield). ^{1}H NMR (500 MHz, $CDCl_3$) δ 8.03 (d, J = 0.7 Hz, 1H), 7.83 (dd, J = 8.6, 1.5 Hz, 1H), 7.72 (d, J = 8.8 Hz, 1H), 7.68 (d, J = 8.6 Hz, 1H), 7.04 (dd, J = 8.8, 2.2 Hz, 1H), 6.86 (d, J = 2.0 Hz, 1H), 4.18 (t, J =

7.5 Hz, 2H), 3.94 (t, J = 5.0 Hz, 4H), 3.23 (t, J = 5.0 Hz, 4H), 2.63 (s, 3H), 1.88 – 1.81 (m, 2H), 0.87 (t, J = 7.4 Hz, 3H). ^{13}C NMR (126 MHz, $CDCl_3$) δ 163.2, 155.5, 152.3, 148.8, 138.0, 136.6, 130.7, 126.7, 123.2, 122.9, 120.4, 114.3, 110.2, 97.1, 67.2 (2 × C), 51.3 (2 × C), 46.4, 23.2, 11.4, 10.2. MS (ESI) *m/z* $[M + H]^+$ calcd 377.19; found 377.1. HPLC, t_R = 9.54 min, 98.79% purity.

7-Bromo-3-methyl-5-(6-morpholino-1-propyl-1*H*-benzo[*d*]imidazol-2-yl)benzo[*d*]isoxazole (7b).

Step 1: To a stirred solution of compound **25a** (6 g, 30.9 mmol) in CH_2Cl_2 (40 mL) was added pyridine (10.0 mL, 123.6 mmol), followed by a dropwise addition of bromine (1.74 mL, 34.0 mmol) in CH_2Cl_2 (10 mL) at 0 °C. The reaction mixture was stirred at room temperature for 2 h. The mixture was then cooled to 5 °C and 4 N HCl (23.2 mL, 92.7 mmol) was added dropwise. The organic layer was separated, dried over Na_2SO_4, and concentrated to afford a brown solid which was then stirred in DCM/petroleum ether (1:1, 30 mL) for 1 h. The solid was collected by filtration and dried to give methyl 3-acetyl-5-bromo-4-hydroxybenzoate (**25b**) as a brown solid (7.6 g, 90% yield). ^{1}H NMR (500 MHz, $CDCl_3$) δ 13.42 (s, 1H), 8.45 (d, J = 1.9 Hz, 1H), 8.42 (d, J = 1.8 Hz, 1H), 3.94 (s, 3H), 2.73 (s, 3H).

Step 2: Methyl 3-bromo-4-hydroxy-5-(1-(hydroxyimino)ethyl)benzoate (**26b**) was prepared from **25b** according to general procedure of step 3 as described for **7a**. White solid, 85% yield. ^{1}H NMR (500 MHz, DMSO-d_6) δ 13.47 (s, 1H), 12.13 (s, 1H), 8.06 (d, J = 1.5 Hz, 1H), 8.05 (d, J = 1.5 Hz, 1H), 3.84 (s, 3H), 2.33 (s, 3H).

Step 3: Methyl 7-bromo-3-methylbenzo[*d*]isoxazole-5-carboxylate (**27b**) was prepared from **26b** according to general procedure of step 4 as described for **7a**. White solid, 78% yield. ^{1}H NMR (500 MHz, $CDCl_3$) δ 8.41 (s, 1H), 8.33 (s, 1H), 3.98 (s, 3H), 2.63 (s, 3H).

Step 4: 7-Bromo-3-methylbenzo[*d*]isoxazole-5-carboxylic acid (**28b**) was prepared from **27b** according to general procedure of step 5 as described for **7a**. White solid, 99% yield. ^{1}H NMR (500 MHz, DMSO-d_6) δ 8.47 (d, J = 1.2 Hz, 1H), 8.32 (d, J = 1.3 Hz, 1H), 2.62 (s, 3H).

Step 5: 7-Bromo-3-methyl-*N*-(4-morpholino-2-(propylamino)phenyl)benzo[*d*]isoxazole-5-carboxamide (**33b**) was prepared from **28b** and **32a** according to general procedure of step 9 as described for **7a**. Yellow solid, 41% yield. ^{1}H NMR (400 MHz, DMSO) δ 9.68 (s, 1H), 8.60 – 8.40 (m, 2H), 6.95 (d, J = 8.1 Hz, 1H), 6.28 – 6.12 (m, 2H), 5.02 – 4.84 (m, 1H), 3.79 – 3.69 (m, 4H), 3.13 – 3.06 (m, 4H), 3.05 – 2.99 (m, 2H), 2.63 (s, 3H), 1.64 – 1.50 (m, 2H), 0.92 (t, J = 6.8 Hz, 3H).

Step 6: The title compound **7b** was prepared from **33b** according to general procedure of step 10 as described for **7a**. White solid, 11% yield. ^{1}H NMR (400 MHz, $CDCl_3$) δ 8.03 (d, J = 1.1 Hz, 1H), 7.95 (d, J = 1.1 Hz, 1H), 7.71 (d, J = 8.8 Hz, 1H), 7.04 (dd, J = 8.8, 2.1 Hz, 1H), 6.85 (d, J = 2.0 Hz, 1H), 4.23 – 4.15 (t, J = 7.6 Hz, 2H), 3.93 (t, J = 4.8 Hz, 4H), 3.23 (t, J = 4.8 Hz, 4H), 2.63 (s, 3H), 1.91 – 1.80 (m, 2H), 0.89 (t, J = 7.4 Hz, 3H). ^{13}C NMR (126 MHz, $CDCl_3$) δ 160.9, 156.3, 150.9, 149.1, 138.0, 136.7, 133.5, 128.5, 124.0, 121.6, 120.6, 114.5, 103.2, 97.0, 67.2 (2 × C), 51.2 (2 × C), 46.5, 23.3, 11.4, 10.5. MS (ESI) *m/z* $[M + H]^+$ calcd 455.10 & 457.10; found 455.3 & 457.5. HPLC, t_R = 13.62 min, 96.09% purity.

5-(1-Butyl-6-morpholino-1*H*-benzo[*d*]imidazol-2-yl)-3-methylbenzo[*d*]isoxazole (7c). Compound **7c** was prepared according to general procedure as described for **7a**. White solid, 31% yield. ^{1}H NMR (500 MHz, $CDCl_3$) δ 8.03 (d, J = 0.7 Hz, 1H), 7.84 (dd, J = 8.6, 1.5 Hz, 1H), 7.71 (d, J = 8.8 Hz, 1H), 7.68 (d, J = 8.6 Hz, 1H), 7.04 (dd, J = 8.8, 2.1 Hz, 1H), 6.86 (d, J = 2.0 Hz, 1H), 4.21 (t, J = 7.5 Hz, 2H), 3.93 (t, J = 5.0 Hz, 4H), 3.23 (t, J = 5.0 Hz, 4H), 2.63 (s, 3H),

1.83 – 1.76 (m, 2H), 1.31 – 1.26 (m, 2H), 0.86 (t, J = 7.4 Hz, 3H). ^{13}C NMR (126 MHz, $CDCl_3$) δ 163.2, 155.5, 152.2, 148.8, 137.9, 136.6, 130.7, 126.6, 123.1, 122.9, 120.4, 114.3, 110.2, 97.0, 67.2 (2 × C), 51.3 (2 × C), 44.6, 31.9, 20.1, 13.7, 10.2. MS (ESI) *m/z* $[M + H]^+$ calcd 391.21; found 391.1. HPLC, t_R = 11.66 min, 97.39% purity.

7-Bromo-5-(1-butyl-6-morpholino-1*H*-benzo[*d*]imidazol-2-yl)-3-methylbenzo[*d*]isoxazole (7d). Compound **7d** was prepared according to general procedure as described for **7b**. White solid, 57% yield. ^{1}H NMR (400 MHz, $CDCl_3$) δ 8.04 (d, J = 1.2 Hz, 1H), 7.96 (d, J = 1.2 Hz, 1H), 7.71 (d, J = 8.8 Hz, 1H), 7.05 (dd, J = 8.8, 2.1 Hz, 1H), 6.85 (d, J = 2.0 Hz, 1H), 4.22 (t, J = 7.6 Hz, 2H), 3.94 (t, J = 4.8 Hz, 4H), 3.23 (t, J = 4.8 Hz, 4H), 2.63 (s, 3H), 1.85 – 1.77 (m, 2H), 1.35 – 1.26 (m, 2H), 0.90 (t, J = 7.3 Hz, 3H). ^{13}C NMR (126 MHz, $CDCl_3$) δ 160.9, 156.3, 150.7, 149.0, 137.9, 136.7, 133.5, 128.4, 123.9, 121.6, 120.6, 114.5, 103.2, 96.9, 67.2 (2 × C), 51.2 (2 × C), 44.6, 31.9, 20.1, 13.7, 10.5. MS (ESI) *m/z* $[M + H]^+$ calcd 469.12 & 471.11; found 469.1 & 471.3. HPLC, t_R = 19.95 min, 96.49% purity.

5-(1-(2-Methoxyethyl)-6-morpholino-1*H*-benzo[*d*]imidazol-2-yl)-3-methylbenzo[*d*]isoxazole (7e). Compound **7e** was prepared according to general procedure as described for **7a**. White solid, 47% yield. ^{1}H NMR (400 MHz, $CDCl_3$) δ 8.20 (d, J = 0.9 Hz, 1H), 8.01 (dd, J = 8.7, 1.6 Hz, 1H), 7.72 (d, J = 8.8 Hz, 1H), 7.66 (d, J = 8.7 Hz, 1H), 7.05 (dd, J = 8.8, 2.2 Hz, 1H), 6.91 (d, J = 2.1 Hz, 1H), 4.37 (t, J = 5.4 Hz, 2H), 3.93 (t, J = 4.8 Hz, 4H), 3.81 (t, J = 5.4 Hz, 2H), 3.31 (s, 3H), 3.23 (t, J = 4.8 Hz, 4H), 2.63 (s, 3H). ^{13}C NMR (126 MHz, $CDCl_3$) δ 163.3, 155.6, 152.9, 148.9, 137.9, 136.8, 131.5, 126.3, 123.5, 123.0, 120.5, 114.4, 110.1, 97.2, 70.8, 67.2 (2 × C), 59.3, 51.3

(2 × C), 45.1, 10.2. MS (ESI) *m/z* $[M + H]^+$ calcd 393.18; found 393.1. HPLC, t_R = 7.62 min, 96.61% purity.

7-Bromo-5-(1-(2-methoxyethyl)-6-morpholino-1*H*-benzo[*d*]imidazol-2-yl)-3-methylbenzo[*d*]isoxazole (7f). Compound **7f** was prepared according to general procedure as described for **7b**. White solid, 35% yield. ^{1}H NMR (400 MHz, $CDCl_3$) δ 8.31 (d, *J* = 0.9 Hz, 1H), 8.19 (d, *J* = 0.9 Hz, 1H), 7.72 (d, *J* = 8.8 Hz, 1H), 7.06 (dd, *J* = 8.8, 2.1 Hz, 1H), 6.87 (d, *J* = 1.9 Hz, 1H), 4.37 (t, *J* = 5.2 Hz, 2H), 3.93 (t, *J* = 4.8 Hz, 4H), 3.85 (t, *J* = 5.2 Hz, 2H), 3.35 (s, 3H), 3.23 (t, *J* = 4.8 Hz, 4H), 2.62 (s, 3H). ^{13}C NMR (126 MHz, $CDCl_3$) δ 160.9, 156.4, 151.5, 149.0, 137.8, 136.7, 134.4, 128.0, 123.7, 122.4, 120.6, 114.6, 102.9, 96.9, 70.6, 67.2 (2 × C), 59.3, 51.1 (2 × C), 45.2, 10.4. MS (ESI) *m/z* $[M + H]^+$ calcd 471.10 & 473.09; found 471.0 & 473.0. HPLC, t_R = 11.55 min, 95.69% purity.

5-(1-(Cyclopropylmethyl)-6-morpholino-1*H*-benzo[*d*]imidazol-2-yl)-3-methylbenzo[*d*]isoxazole (7g). Compound **7g** was prepared according to general procedure as described for **7a**. White solid, 30% yield. ^{1}H NMR (400 MHz, $CDCl_3$) δ 8.05 (d, *J* = 0.7 Hz, 1H), 7.85 (dd, *J* = 8.6, 1.5 Hz, 1H), 7.72 (d, *J* = 8.8 Hz, 1H), 7.68 (d, *J* = 8.6 Hz, 1H), 7.05 (dd, *J* = 8.8, 2.2 Hz, 1H), 6.94 (d, *J* = 2.0 Hz, 1H), 4.11 (d, *J* = 6.5 Hz, 2H), 3.94 (t, *J* = 4.8 Hz, 4H), 3.23 (t, *J* = 4.8 Hz, 4H), 2.63 (s, 3H), 1.21 – 1.13 (m, 1H), 0.53 (q, *J* = 5.8 Hz, 2H), 0.16 (q, *J* = 5.1 Hz, 2H). ^{13}C NMR (126 MHz, $CDCl_3$) δ 163.2, 155.5, 152.3, 148.8, 137.9, 136.8, 130.9, 126.7, 123.1, 123.0, 120.4, 114.4, 110.2, 97.3, 67.2 (2 × C), 51.3 (2 × C), 49.0, 11.4, 10.3, 4.6 (2 × C). MS (ESI) *m/z* $[M + H]^+$ calcd 389.19; found 389.1. HPLC, t_R = 9.54 min, 96.51% purity.

7-Bromo-5-(1-(cyclopropylmethyl)-6-morpholino-1*H*-benzo[*d*]imidazol-2-yl)-3-methylbenzo[*d*]isoxazole (7h). Compound **7h** was prepared according to general procedure as described for **7b**. White solid, 37% yield. ^{1}H NMR (400 MHz, $CDCl_3$) δ 8.06 (d, *J* = 1.1 Hz, 1H), 7.98 (d, *J* = 1.0 Hz, 1H), 7.71 (d, *J* = 8.8 Hz, 1H), 7.05 (dd, *J* = 8.8, 2.1 Hz, 1H), 6.93 (d, *J* = 2.0 Hz, 1H), 4.12 (d, *J* = 6.4 Hz, 2H), 3.94 (t, *J* = 4.8 Hz, 4H), 3.24 (t, *J* = 4.8 Hz, 4H), 2.63 (s, 3H), 1.22 – 1.13 (m, 1H), 0.58 (q, *J* = 5.5 Hz, 2H), 0.21 (q, *J* = 5.2 Hz, 2H). ^{13}C NMR (126 MHz, $CDCl_3$) δ 160.9, 156.3, 150.8, 149.0, 137.8, 136.9, 133.7, 128.4, 123.9, 121.8, 120.5, 114.6, 103.1, 97.2, 67.2 (2 × C), 51.2 (2 × C), 49.1, 11.4, 10.5, 4.7 (2 × C). MS (ESI) *m/z* $[M + H]^+$ calcd 467.10 & 469.10; found 467.0 & 469.0. HPLC, t_R = 15.35 min, 96.73% purity.

5-(1-(Sec-butyl)-6-morpholino-1*H*-benzo[*d*]imidazol-2-yl)-3-methylbenzo[*d*]isoxazole (7i).

Step 1: Compound **28a** (199 mg, 1.12 mmol), N^1-(sec-butyl)-5-morpholinobenzene-1,2-diamine (279.3 mg, 1.12 mmol), 2-chloro-1-methylpyridinium iodide (687.2 mg, 2.69 mmol) and tributylamine (966.4 mg, 5.38 mmol) were dissolved in toluene (15 mL). The reaction mixture was stirred under N_2 atmosphere for 16 h at 90 °C. Afterwards the solvent was evaporated. The residue was extracted with EtOAc (3 × 20 mL) and washed with brine. The organic phase was dried over Na_2SO_4 and concentrated under reduced pressure. The crude product was purified by silica gel chromatography to give *N*-(2-(sec-butylamino)-4-morpholinophenyl)-3-methylbenzo[*d*]isoxazole-5-carboxamide (**33i**) as a white solid (63 mg, 14% yield). ^{1}H NMR (400 MHz, DMSO-d_6) δ 9.64 (s, 1H), 8.52 (s, 1H), 8.24 (d, *J* = 8.8 Hz, 1H), 7.80 (d, *J* = 8.8 Hz, 1H), 6.97 (d, *J* = 8.1 Hz, 1H), 6.30 – 6.15 (m, 2H), 4.42 (d, *J* = 7.8 Hz, 1H), 3.74 (t, *J* = 4.8 Hz, 4H), 3.51 – 3.35 (m, 1H), 3.08 (t, *J* = 4.8 Hz, 4H), 2.62 (s, 3H), 1.60 – 1.47 (m, 1H), 1.47 – 1.37 (m, 1H), 1.11 (d, *J* = 6.3 Hz, 3H), 0.89 (t, *J* = 7.4 Hz, 3H).

Step 2: The title compound **7i** was prepared from **33i** according to general procedure of step 10 as described for **7a**. White solid, 42% yield. ^{1}H NMR (400 MHz, $CDCl_3$) δ 7.96 (s, 1H), 7.76 – 7.70 (m, 2H), 7.67 (d, *J* = 8.6 Hz, 1H), 7.03 (d, *J* = 8.4 Hz, 2H), 4.48 – 4.39 (m, 1H), 3.93 (t, *J* = 4.8 Hz, 4H), 3.21 (t, *J* = 4.8 Hz, 4H), 2.63 (s, 3H), 2.25 – 2.14 (m, 1H), 1.93 – 1.82 (m, 1H), 1.70 (d, *J* = 7.0 Hz, 3H), 0.67 (t, *J* = 7.3 Hz, 3H). ^{13}C NMR (126 MHz, $CDCl_3$) δ 163.2, 155.5, 153.0, 148.22, 138.7, 134.5, 131.0, 127.0, 123.2, 123.1, 120.7, 114.2, 110.1, 99.4, 67.2 (2 × C), 55.0, 51.4 (2 × C), 28.1, 20.0, 11.3, 10.2. MS (ESI) *m/z* $[M + H]^+$ calcd 391.49; found 391.4. HPLC, t_R = 10.64 min, 99.11% purity.

5-(1-Benzyl-6-morpholino-1*H*-benzo[*d*]imidazol-2-yl)-3-methylbenzo[*d*]isoxazole (7j). Compound **7j** was prepared according to general procedure as described for **7i**. White solid, 52% yield. ^{1}H NMR (400 MHz, $CDCl_3$) δ 7.91 ((d, *J* = 0.7 Hz, 1H), 7.80 (dd, *J* = 8.8, 1.6 Hz, 1H), 7.77 (d, *J* = 9.0 Hz, 1H), 7.57 (d, *J* = 8.7 Hz, 1H), 7.43 – 7.30 (m, 3H), 7.15 (d, *J* = 6.6 Hz, 2H), 7.06 (dd, *J* = 8.8, 2.2 Hz, 1H), 6.71 (d, *J* = 2.1 Hz, 1H), 5.40 (s, 2H), 3.87 (t, *J* = 4.8 Hz, 4H), 3.14 (t, *J* = 4.8 Hz, 4H), 2.49 (s, 3H). ^{13}C NMR (126 MHz, $CDCl_3$) δ 163.3, 155.5, 152.7, 149.1, 137.9, 137.5, 136.7, 130.8, 129.4 (2 × C), 128.1, 126.1 (2 × C), 126.0, 123.0, 122.7, 120.5, 114.4, 110.3, 96.9, 67.1 (2 × C), 51.0 (2 × C), 48.5, 10.1. MS (ESI) *m/z* $[M + H]^+$ calcd 425.50; found 425.5. HPLC, t_R = 10.38 min, 98.94% purity.

5-(1-(Cyclohexylmethyl)-6-morpholino-1*H*-benzo[*d*]imidazol-2-yl)-3-methylbenzo[*d*]isoxazole (7k). Compound **7k** was prepared according to general procedure as described for **7a**. White solid, 34% yield. ^{1}H NMR (400 MHz, $CDCl_3$) δ 8.00 (d, *J* = 0.9 Hz, 1H), 7.82 (dd, *J* = 8.6, 1.6 Hz, 1H), 7.70 (d, *J* = 8.8 Hz, 1H), 7.67 (d, *J* = 8.6 Hz, 1H), 7.03 (dd, *J* =

8.8, 2.2 Hz, 1H), 6.84 (d, *J* = 2.1 Hz, 1H), 4.08 (d, *J* = 7.4 Hz, 2H), 3.94 (t, *J* = 4.8 Hz, 4H), 3.23 (t, *J* = 4.8 Hz, 4H), 2.63 (s, 3H), 1.82 – 1.72 (m, 1H), 1.61 – 1.51 (m, 3H), 1.45 (d, *J* = 12.6 Hz, 2H), 1.12 – 0.98 (m, 3H), 0.81 – 0.69 (m, 2H). ^{13}C NMR (126 MHz, $CDCl_3$) δ 163.2, 155.5, 152.7, 148.7, 137.9, 136.9, 131.0, 127.0, 123.1, 123.0, 120.4, 114.2, 110.2, 97.5, 67.2 (2 × C), 51.3 (2 × C), 51.0, 38.2, 31.0 (2 × C), 26.1, 25.6 (2 × C), 10.3. MS (ESI) *m/z* $[M + H]^+$ calcd 431.24; found 431.1. HPLC, t_R = 20.92 min, 98.48% purity.

7-Bromo-5-(1-(cyclohexylmethyl)-6-morpholino-1*H*-benzo[*d*]imidazol-2-yl)-3-methylbenzo[*d*]isoxazole (7l). Compound **7l** was prepared according to general procedure as described for **7b**. White solid, 46% yield. ^{1}H NMR (400 MHz, $CDCl_3$) δ 8.02 (d, *J* = 1.2 Hz, 1H), 7.94 (d, *J* = 1.2 Hz, 1H), 7.70 (d, *J* = 8.8 Hz, 1H), 7.04 (dd, *J* = 8.8, 2.1 Hz, 1H), 6.84 (d, *J* = 2.0 Hz, 1H), 4.09 (d, *J* = 7.3 Hz, 2H), 3.94 (t, *J* = 4.8 Hz, 4H), 3.24 (t, *J* = 4.8 Hz, 4H), 2.64 (s, 3H), 1.82 – 1.76 (m, 1H), 1.62 – 1.55 (m, 3H), 1.47 (d, *J* = 12.8 Hz, 2H), 1.14 – 1.00 (m, 3H), 0.83 – 0.74 (m, 2H). ^{13}C NMR (126 MHz, $CDCl_3$) δ 160.8, 156.3, 151.2, 149.0, 137.9, 137.0, 133.7, 128.8, 123.9, 121.7, 120.6, 114.4, 103.2, 97.4, 67.2 (2 × C), 51.2 (2 × C), 51.1, 38.4, 31.1 (2 × C), 26.1, 25.9 (2 × C), 10.5. MS (ESI) *m/z* $[M + H]^+$ calcd 509.15 and 511.15; found 509.1 and 511.1. HPLC, t_R = 35.13 min, 98.97% purity.

(S)-5-(1-(Cyclohexylmethyl)-6-(3-methylmorpholino)-1*H*-benzo[*d*]imidazol-2-yl)-3-methylbenzo[*d*]isoxazole (7m). Compound **7m** was prepared according to general procedure as described for **7a**. White solid, 60% yield. ^{1}H NMR (500 MHz, $CDCl_3$) δ 8.01 (s, 1H), 7.83 (dd, *J* = 8.6, 1.5 Hz, 1H), 7.72 (d, *J* = 8.7 Hz, 1H), 7.68 (d, *J* = 8.6 Hz, 1H), 7.07 (dd, *J* = 8.7, 2.0 Hz, 1H), 6.93 (d, *J* = 1.8 Hz, 1H), 4.09 (d, *J* = 7.3 Hz, 2H), 4.01 – 3.97 (m, 1H), 3.96 – 3.92 (m, 1H),

3.87 – 3.82 (m, 1H), 3.69 – 3.62 (m, 2H), 3.24 – 3.19 (m, 1H), 3.14 – 3.09 (m, 1H), 2.64 (s, 3H), 1.81 – 1.72 (m, 1H), 1.60 – 1.53 (m, 3H), 1.45 (t, J = 11.7 Hz, 2H), 1.12 – 1.04 (m, 3H), 1.03 (d, J = 6.2 Hz, 3H), 0.79 – 0.72 (m, 2H). ^{13}C NMR (126 MHz, $CDCl_3$) δ 163.2, 155.5, 152.9, 147.3, 138.7, 137.0, 131.0, 127.1, 123.2, 123.0, 120.4, 116.2, 110.2, 101.2, 72.7, 67.6, 53.5, 51.0, 48.7, 38.4, 31.0, 31.0, 26.2, 25.7, 25.7, 12.8, 10.2. MS (ESI) *m/z* $[M + H]^+$ calcd 445.25; found 445.2. HPLC, t_R = 19.41 min, 99.47% purity.

(S)-7-Bromo-5-(1-(cyclohexylmethyl)-6-(3-methylmorpholino)-1*H*-benzo[*d*]imidazol-2-yl)-3-methylbenzo[*d*]isoxazole (7n). Compound **7n** was prepared according to general procedure as described for **7b**. White solid, 16% yield. ^{1}H NMR (500 MHz, $CDCl_3$) δ 8.03 (s, 1H), 7.95 (s, 1H), 7.71 (d, J = 8.7 Hz, 1H), 7.07 (d, J = 8.7 Hz, 1H), 6.92 (s, 1H), 4.09 (d, J = 7.2 Hz, 2H), 4.01 – 3.98 (m, 1H), 3.95 (d, J = 8.6 Hz, 1H), 3.84 (t, J = 8.3 Hz, 1H), 3.69 – 3.66 (m, 2H), 3.22 (t, J = 8.5 Hz, 1H), 3.13 – 3.10 (m, 1H), 2.64 (s, 3H), 1.83 – 1.73 (m, 1H), 1.62 – 1.56 (m, 3H), 1.47 (t, J = 11.1 Hz, 2H), 1.14 – 1.05 (m, 3H), 1.04 (d, J = 5.7 Hz, 3H), 0.85 – 0.74 (m, 2H). ^{13}C NMR (126 MHz, $CDCl_3$) δ 160.8, 156.4, 151.4, 147.5, 138.4, 137.0, 133.6, 128.7, 123.9, 121.7, 120.5, 116.1, 103.2, 100.8, 72.6, 67.5, 53.3, 51.1, 48.2, 38.5, 31.1, 31.0, 26.1, 25.7, 25.7, 12.7, 10.5. MS (ESI) *m/z* $[M + H]^+$ calcd 523.16 and 525.16; found 523.0 and 525.0. HPLC, t_R = 3.83 min, 98.68% purity.

5.3. Biological Evaluation.

5.3.1. Protein Expression and Purification.

Bromodomain containing proteins expression and purification were carried out as previously described.[23] (For details, see Supporting Information)

5.3.2. Thermal Shift Assay (ΔT_m).

Bromodomain thermal shift (ΔT_m) assays were carried out as previously described.[23] (For details, see Supporting Information)

5.3.3. AlphaScreen Assay.

Bromodomain AlphaScreen assays were carried out as previously described.[23] (For details, see Supporting Information)

5.3.4. Isothermal Titration Calorimetry (ITC).

The ITC measurements were carried out using an ITC200 instrument (Microcal, GE Healthcare). All experiments were performed at 25 °C while stirring at 1,000 rpm in an ITC buffer (25 mM HEPES, 150 mM NaCl, 0.5 mM TCEP, 5% glycerol and pH 7.5). All titrations of bromodomain containing proteins into ligands were performed using an initial injection of 0.5 μL followed by 20 identical injections of 2 μL with a duration of 4 seconds per injection and a spacing of 180 seconds between injections. The stock solutions of ligands and the bromodomain containing proteins were diluted with the ITC buffer to a compound concentration of 40-60 μM and protein concentration of 500-600 μM before titrations. The final concentration of DMSO in the reaction buffer is less than 0.25% of the total volume. In order to estimate the background of the heat of dilution for the proteins, the proteins were titrated into ITC buffer on separate experiments. Data was corrected for heats of dilution by subtracting the data from independent titrations of proteins into buffer. In all the cases, a single binding site mode was employed and a nonlinear least-squares algorithm was used to obtain best-fit values of the stoichiometry (n), change in enthalpy (ΔH), and binding constant (K_d). Thermodynamic parameters were subsequently calculated with

the formula $\Delta G = \Delta H - T\Delta S = -RTlnK$, where ΔG, ΔH, ΔS, T, and R are the changes in free energy, enthalpy, entropy of binding, experimental temperature, the gas constant, respectively. Dissociation constants and thermodynamic parameters are listed in Table 4. Titrations were run in triplicate to ensure reproducibility. MicroCal™ Origin7 software was used to collect and process the data.

5.3.5. Crystallization, Data Collection, and Structure Determination.

The purified and concentrated (10-15 mg/mL) BRD4(1) protein was incubated with ligands at a molar ratio of 1:3 for 40 minutes on ice. All crystallizations were carried out using the sitting drop vapor diffusion method in 24-well plate at 4 °C. Crystals of BRD4(1) with ligands were grown by mixing 1 μL of the protein (8-15 mg/mL) with 1 μL of reservoir solution containing various well buffer. Crystals of BRD4(1) with **5t**, **6a**, **6e**, **6f**, **6i**, **6j**, **6m** were grown with reservoir solution containing 0.2 M $NaNO_3$, 0.1 M HEPES, pH 7.0-8.5, 20% PEG3350 and 10% ethylene glycol.

Most crystals appeared in 2 days and grew to full size approximately one week. Crystals were cryo-protected using the well solution supplemented with additional ethylene glycol and were flash frozen in liquid nitrogen. All diffraction data were collected on beamlines BL17U and BL19U1 at Shanghai Synchrotron Radiation Facilities (SSRF) at 100 K. Data sets were processed (indexing and integration) using the program MOSFLM[41] and scaled using Aimless from the Collaborative Computational Project 4 (CCP4) program suite.[42] Molecular replacement was performed with the CCP4 program Phaser[43] using BRD4(1)-JQ1 complex structure (PDB code: 3MXF) as a search model. The model was refined using CCP4 program REFMAC5[44] and

rebuilt with COOT.[45] The quality of the models was checked using MolProbity.[46] Structure figures were prepared using the program PyMOL. The statistics of data collection and the model refinement are summarized in Supporting Information Table S1. Crystals of **5t**, **6a**, **6f**, **6i**, **6j**, and **6m** with BRD4(1) diffracted to resolutions of 1.84, 1.76, 1.62, 1.87, 2.00, and 1.42 Å, respectively. The coordinates were deposited in the PDB with the following IDs: 5Y8Z for compound **5t**, 5Y8W for compound **6a**, 5Y93 for compound **6f**, 5Y8Y for compound **6i**, 5Y94 for compound **6j**, 5Y8C for compound **6m**.

5.3.6. Cell Viability and Cell Colony Formation Assays.

LNCaP, C4-2B, 22Rv1 and VCaP prostate cancer cells were cultured in RPMI1640 with 10% FBS at 37 °C and an atmosphere of 5% CO_2. For cell viability, cells were seeded in 384-well plates at 500−1000 cells per well (optimum density for growth) in a total volume of 20 μL of media. After 12 h, 10 μL chemical compounds with 2-fold or 3-fold serial dilution was added to each well with final concentration from 5 nM to 100 μM. The measurement was conducted 96 h after seeded for LNCaP, C4-2B, and 22Rv1, and 144 h after seeded for VCaP. Then, 25 μL of CellTiter-GLO reagents (Promega) was added, and luminescence was measured on GLOMAX microplate luminometer (Promega), according to the manufacturer's instructions. The estimated *in vitro* half-maximal inhibitory concentration (IC_{50}) values were calculated using GraphPad Prism 6 software. Further experimental details for other cell lines are provided in Supporting Information.

For long-term colony formation assay, 2000 cells per well were seeded in 6-well plates and treated with vehicle or 0.5 μM, 1 μM or 2 μM of compound **6i** or **7m**. After 14 days, cells were fixed with methanol, stained with crystal violet and photographed.

5.3.7. Analysis of mRNA Expression in Cells.

LNCaP and VCaP cells were plated at 1.5×10^5 cells per well in 12-well plates. 24 h later, cells were treated with vehicle, JQ1 (**1**) (5 μM), **6i** (5 μM) or **7m** (5 μM) for 48 h. Total RNA was extracted by Eastep® Super Total RNA Extraction Kit and reverse transcribed using All-in-one™ First-Strand cDNA Synthesis Kit. Quantitative real time PCR (qRT-PCR) was performed in triplicate using standard SYBR green reagents on a Bio-Rad CFX96 Real-Time PCR system. Analysis was performed on triplicate PCR data for each biological duplicate (normalized to β−actin). The primer sequences for qPCR used are as follows: *AR-FL-fwd*, CAG TGG ATG GGC TGA AAA AT; *AR-FL_rev*, GGA GCT TGG TGA GCT GGT AG; *AR-V7_fwd*, CAG GGA TGA CTC TGG GAG AA; *AR-V7_rev*, GCC CTC TAG AGC CCT CAT TT; *PSA_fwd*, CAC AGG CCA GGT ATT TCA GGT; *PSA_rev*, GAG GCT CAT ATC GTA GAG CGG; *KLK2_fwd*, CAA CAT CTG GAG GGG AAA GGG; *KLK2_rev*, AGG CCA AGT GAT GCC AGA AC; *TMPRSS2_fwd*, CAA GTG CTC CAA CTC TGG GAT; *TMPRSS2_rev*, AAC ACA CCG ATT CTC GTC CTC; *ERG_fwd*, CGC AGA GTT ATC GTG CCA GCA GAT; *ERG_rev*, CCA TAT TCT TTC ACC GCC CAC TCC; *C-MYC_fwd*, GGC TCC TGG CAA AAG GTC A; *C-MYC*_rev, CTG CGT AGT TGT GCT GAT GT; *β-Actin_fwd*, GAG AAA ATC TGG CAC CAC ACC; *β-Actin_rev*, ATA CCC CTC GTA GAT GGG CAC.

5.3.8. PSA Luciferase Reporter Gene Assay.

LNCaP cells were seeded in 24-well plates and transiently transfected using Lipofectamine 3000 (Invitrogen) according to the manufacturer's instructions. 200 ng PSA-Luc plasmid (PSA promoter driven luciferase reporter plasmid, a gift from Dr. H. Eric Xu) and 10 ng renilla luciferase expression plasmid per well were cotransfected into LNCaP cells. Compounds were added 24 h after transfection. The cells were harvested after another 24 h for a luciferase assay using the dual-luciferase reporter assay system (Promega). Luciferase activities were normalized to renilla activity, which was co-transfected as an internal control. All of the assays were performed in triplicate, and the standard deviations were calculated accordingly.

5.3.9. In vivo Efficacy Studies in C4-2B Xenograft Model in Mice.

Four-week-old male mice (strain: C.B-17/IcrHsd-*Prkdc*^{scid} for C4-2B) were purchased from Envigo, Inc and used for tumor inoculation. Each mouse was inoculated subcutaneously at the dorsal flank on both sides of the mice with C4-2B tumor cells (2×10^6 cells) in a mixture of 100 μL PBS and Matrigel (1:1). When the tumor volume reached approximately 100 mm^3, the mice were randomized into groups (n = 5 to 7 per group) and then treated intraperitoneally (i.p.) with 100 μL of either vehicle or **6i** and **7m** (in a formulation of 15% Cremophor EL, Calbiochem, 82.5% PBS and 2.5% dimethyl sulfoxide (DMSO)) for five times per week. The length (L) and width (W) of the tumor mass were monitored by calipers, and volume was expressed in mm^3 calculated with the equation: $V = \pi/6 \times (L \times W^2)$. Tumor growth inhibition (TGI) was calculated using the equation: $TGI = [1 - (T - T_0)/(C - C_0)] \times 100$, wherein, T and T_0 are the mean tumor volumes on a specific experimental day and on the first day of treatment, respectively, for the test groups; and likewise C and C_0 are the mean tumor volumes for the vehicle group. The

procedures were approved by the Institutional Animal Care and Use Committee of the University of California, Davis.

ASSOCIATED CONTENT

Supporting Information

Table S1-S3, Figure S1-S6. Experimental Procedures for Protein Expression and Purification, Thermal Shift Assay, AlphaScreen Assay, BROMOscan Assay, Cell Viability Assays, Western Blot Analysis and Pharmacokinetics Analysis (PDF). ^{1}H-NMR and ^{13}C-NMR spectra of the synthesized compounds (PDF) and molecular formula strings for compounds with associated biological data (CSV). The Supporting Information is available free of charge on the ACS Publications website at DOI:

Accession Code

Coordinates for compounds **5t** (PDB code 5Y8Z), **6a** (PDB code 5Y8W), **6f** (PDB code 5Y93), **6i** (PDB code 5Y8Y), **6j** (PDB code 5Y94), **6m** (PDB code 5Y8C) in complex with BRD4(1) have been deposited into the Protein Data Bank. Authors will release the atomic coordinates and experimental data upon article publication.

AUTHOR INFORMATION

Corresponding Author

*E-mail: xu_yong@gibh.ac.cn. Phone: +86-20-32093612.

Author Contributions

#These authors contributed equally.

ORCID

Yong Xu: 0000-0003-3601-0246

Notes

The authors declare no competing financial interest.

ACKNOWLEDGMENT

We gratefully acknowledge financial support from the National Natural Science Foundation of China (grant No. 81673357, No. 21602222), the "Personalized Medicines − Molecular Signature-based Drug Discovery and Development", Strategic Priority Research Program of the Chinese Academy of Sciences (grant No. XDA12020315 and XDA12010363), the Chinese National Programs for Key Research and Development (grant No. 2016YFB0201701), the International collaborative funds from Guangdong Province (grant No. 2016A050502035), the Natural Science Foundation of Guangdong Province (grant No. 2015A030312014), the Guangzhou Municipal Bureau of Science and Technology (2016201604030030), the US NIH (grant No. R01CA206222) and the Movember Foundation and Prostate Cancer Foundation Challenge Award (grant No. 16CHAL02). The authors thank the staffs from BL17U1, BL18U, BL19U1 beamlines of National Facility for Protein Science Shanghai (NFPS) at Shanghai Synchrotron Radiation Facility, for assistance during data collection. The authors gratefully acknowledge support from the Guangzhou Branch of the Supercomputing Center of Chinese Academy of Sciences.

ABBREVIATIONS

BRD, bromodomain; BET, bromodomain and extraterminal domain; SAR, structure activity relationship; TSA, thermal shift assay; PCa, prostate cancer; CRPC, castration-resistant prostate cancer; PSA, prostatic specific antigen; Enz, Enzalutamide; Abi, Abiraterone

REFERENCES

(1) Ferlay, J.; Steliarova-Foucher, E.; Lortet-Tieulent, J.; Rosso, S.; Coebergh, J. W.; Comber, H.; Forman, D.; Bray, F. Cancer incidence and mortality patterns in Europe: estimates for 40 countries in 2012. *Eur. J. Cancer* **2013**, *49*, 1374-1403.

(2) Siegel, R.; Ma, J. M.; Zou, Z. H.; Jemal, A. Cancer statistics, 2014. *CA. Cancer J. Clin.* **2014**, *64*, 9-29.

(3) Torre, L. A.; Bray, F.; Siegel, R. L.; Ferlay, J.; Lortet-Tieulent, J.; Jemal, A. Global cancer statistics, 2012. *CA. Cancer J. Clin.* **2015**, *65*, 87-108.

(4) Katsogiannou, M.; Ziouziou, H.; Karaki, S.; Andrieu, C.; Henry de Villeneuve, M.; Rocchi, P. The hallmarks of castration-resistant prostate cancers. *Cancer Treat. Rev.* **2015**, *41*, 588-597.

(5) Valenca, L. B.; Sweeney, C. J.; Pomerantz, M. M. Sequencing current therapies in the treatment of metastatic prostate cancer. *Cancer Treat. Rev.* **2015**, *41*, 332-340.

(6) Wyatt, A. W.; Gleave, M. E. Targeting the adaptive molecular landscape of castration-resistant prostate cancer. *EMBO Mol. Med.* **2015**, *7*, 878-894.

(7) Antonarakis, E. S.; Lu, C.; Wang, H.; Luber, B.; Nakazawa, M.; Roeser, J. C.; Chen, Y.; Mohammad, T. A.; Chen, Y.; Fedor, H. L.; Lotan, T. L.; Zheng, Q.; De Marzo, A. M.; Isaacs, J. T.; Isaacs, W. B.; Nadal, R.; Paller, C. J.; Denmeade, S. R.; Carducci, M. A.; Eisenberger, M. A.; Luo, J. AR-V7 and resistance to enzalutamide and abiraterone in prostate cancer. *N. Engl. J. Med.* **2014**, *371*, 1028-1038.

(8) Buttigliero, C.; Tucci, M.; Bertaglia, V.; Vignani, F.; Bironzo, P.; Maio, M. D.; Scagliotti, G. V. Understanding and overcoming the mechanisms of primary and acquired resistance to abiraterone and enzalutamide in castration resistant prostate cancer. *Cancer Treat. Rev.* **2015**, *41*, 884-892.

(9) Coleman, D. J.; Van Hook, K.; King, C. J.; Schwartzman, J.; Lisac, R.; Urrutia, J.; Sehrawat, A.; Woodward, J.; Wang, N. J.; Gulati, R.; Thomas, G. V.; Beer, T. M.; Gleave, M.; Korkola, J. E.; Gao, L. N.; Heiser, L. M.; Alumkal, J. J. Cellular androgen content influences enzalutamide agonism of F877L mutant androgen receptor. *Oncotarget* **2016**, *7*, 40690-40703.

(10) Dawson, M. A.; Prinjha, R. K.; Dittmann, A.; Giotopoulos, G.; Bantscheff, M.; Chan, W.-I.; Robson, S. C.; Chung, C.-W.; Hopf, C.; Savitski, M. M.; Huthmacher, C.; Gudgin, E.; Lugo, D.; Beinke, S.; Chapman, T. D.; Roberts, E. J.; Soden, P. E.; Auger, K. R.; Mirguet, O.; Doehner, K.; Delwel, R.; Burnett, A. K.; Jeffrey, P.; Drewes, G.; Lee, K.; Huntly, B. J.; Kouzarides, T. Inhibition of BET recruitment to chromatin as an effective treatment for MLL-fusion leukaemia. *Nature* **2011**, *478*, 529-533.

(11) Zuber, J.; Shi, J. W.; Wang, E.; Rappaport, A. R.; Herrmann, H.; Sison, E. A.; Magoon, D.; Qi, J.; Blatt, K.; Wunderlich, M.; Taylor, M. J.; Johns, C.; Chicas, A.; Mulloy, J. C.; Kogan, S. C.; Brown, P.; Valent, P.; Bradner, J. E.; Lowe, S. W.; Vakoc, C. R. RNAi screen identifies Brd4 as a therapeutic target in acute myeloid leukaemia. *Nature* **2011**, *478*, 524-528.

(12) Asangani, I. A.; Dommeti, V. L.; Wang, X. J.; Malik, R.; Cieslik, M.; Yang, R. D.; Escara-Wilke, J.; Wilder-Romans, K.; Dhanireddy, S.; Engelke, C.; Iyer, M. K.; Jing, X. J.; Wu, Y. M.; Cao, X. H.; Qin, Z. S.; Wang, S. M.; Feng, F. Y.; Chinnaiyan, A. M. Therapeutic targeting of BET bromodomain proteins in castration-resistant prostate cancer. *Nature* **2014**, *510*, 278-282.

(13) Asangani, I. A.; Wilder-Romans, K.; Dommeti, V. L.; Krishnamurthy, P. M.; Apel, I. J.; Escara-Wilke, J.; Plymate, S. R.; Navone, N. M.; Wang, S. M.; Feng, F. Y.; Chinnaiyan, A. M. BET bromodomain inhibitors enhance efficacy and disrupt resistance to AR antagonists in the treatment of prostate cancer. *Mol. Cancer Res.* **2016**, *14*, 324-331.

(14) Sahai, V.; Redig, A. J.; Collier, K. A.; Eckerdt, F. D.; Munshi, H. G. Targeting BET

bromodomain proteins in solid tumors. *Oncotarget* **2016**, *7*, 53997-54009.

(15) Shu, S. K.; Lin, C. Y.; He, H. H.; Witwicki, R. M.; Tabassum, D. P.; Roberts, J. M.; Janiszewska, M.; Huh, S. J.; Liang, Y.; Ryan, J.; Doherty, E.; Mohammed, H.; Guo, H.; Stover, D. G.; Ekram, M. B.; Peluffo, G.; Brown, J.; D'Santos, C.; Krop, I. E.; Dillon, D.; McKeown, M.; Ott, C.; Qi, J.; Ni, M.; Rao, P. K.; Duarte, M.; Wu, S. Y.; Chiang, C. M.; Anders, L.; Young, R. A.; Winer, E. P.; Letai, A.; Barry, W. T.; Carroll, J. S.; Long, H. W.; Brown, M.; Liu, X. S.; Meyer, C. A.; Bradner, J. E.; Polyak, K. Response and resistance to BET bromodomain inhibitors in triple-negative breast cancer. *Nature* **2016**, *529*, 413-417.

(16) Huang, B.; Yang, X. D.; Zhou, M. M.; Ozato, K.; Chen, L. F. Brd4 coactivates transcriptional activation of NF-κB via specific binding to acetylated RelA. *Mol. Cell. Biol.* **2009**, *29*, 1375-1387.

(17) Nicodeme, E.; Jeffrey, K. L.; Schaefer, U.; Beinke, S.; Dewell, S.; Chung, C.-W.; Chandwani, R.; Marazzi, I.; Wilson, P.; Coste, H.; White, J.; Kirilovsky, J.; Rice, C. M.; Lora, J. M.; Prinjha, R. K.; Lee, K.; Tarakhovsky, A. Suppression of inflammation by a synthetic histone mimic. *Nature* **2010**, *468*, 1119-1123.

(18) Filippakopoulos, P.; Qi, J.; Picaud, S.; Shen, Y.; Smith, W. B.; Fedorov, O.; Morse, E. M.; Keates, T.; Hickman, T. T.; Felletar, I.; Philpott, M.; Munro, S.; McKeown, M. R.; Wang, Y.; Christie, A. L.; West, N.; Cameron, M. J.; Schwartz, B.; Heightman, T. D.; La Thangue, N.; French, C. A.; Wiest, O.; Kung, A. L.; Knapp, S.; Bradner, J. E. Selective inhibition of BET bromodomains. *Nature* **2010**, *468*, 1067-1073.

(19) Wyce, A.; Degenhardt, Y.; Bai, Y. C.; Le, B. C.; Korenchuk, S.; Crouthamel, M. C.; McHugh, C. F.; Vessella, R.; Creasy, C. L.; Tummino, P. J.; Barbash, O. Inhibition of BET bromodomain proteins as a therapeutic approach in prostate cancer. *Oncotarget* **2013**, *4*, 2419-

2429.

(20) Chaidos, A.; Caputo, V.; Gouvedenou, K.; Liu, B.; Marigo, I.; Chaudhry, M. S.; Rotolo, A.; Tough, D. F.; Smithers, N. N.; Bassil, A. K.; Chapman, T. D.; Harker, N. R.; Barbash, O.; Tummino, P.; Al-Mahdi, N.; Haynes, A. C.; Cutler, L.; Le, B.; Rahemtulla, A.; Roberts, I.; Kleijnen, M.; Witherington, J. J.; Parr, N. J.; Prinjha, R. K.; Karadimitris, A. Potent antimyeloma activity of the novel bromodomain inhibitors I-BET151 and I-BET762. *Blood* **2014**, *123*, 697-705.

(21) Mirguet, O.; Gosmini, R.; Toum, J.; Clement, C. A.; Barnathan, M.; Brusq, J. M.; Mordaunt, J. E.; Grimes, R. M.; Crowe, M.; Pineau, O.; Ajakane, M.; Daugan, A.; Jeffrey, P.; Cutler, L.; Haynes, A. C.; Smithers, N. N.; Chung, C. W.; Bamborough, P.; Uings, I. J.; Lewis, A.; Witherington, J.; Parr, N.; Prinjha, R. K.; Nicodeme, E. Discovery of epigenetic regulator I-BET762: lead optimization to afford a clinical candidate inhibitor of the BET bromodomains. *J. Med. Chem.* **2013**, *56*, 7501-7515.

(22) Seal, J.; Lamotte, Y.; Donche, F.; Bouillot, A.; Mirguet, O.; Gellibert, F.; Nicodeme, E.; Krysa, G.; Kirilovsky, J.; Beinke, S.; McCleary, S.; Rioja, I.; Bamborough, P.; Chung, C. W.; Gordon, L.; Lewis, T.; Walker, A. L.; Cutler, L.; Lugo, D.; Wilson, D. M.; Witherington, J.; Lee, K.; Prinjha, R. K. Identification of a novel series of BET family bromodomain inhibitors: binding mode and profile of I-BET151 (GSK1210151A). *Bioorg. Med. Chem. Lett.* **2012**, *22*, 2968-2972.

(23) Xue, X. Q.; Zhang, Y.; Liu, Z. X.; Song, M.; Xing, Y. L.; Xiang, Q. P.; Wang, Z.; Tu, Z. C.; Zhou, Y. L.; Ding, K.; Xu, Y. Discovery of benzo[cd]indol-2(1H)-ones as potent and specific BET bromodomain inhibitors: structure-based virtual screening, optimization, and biological evaluation. *J. Med. Chem.* **2016**, *59*, 1565-1579.

(24) Faivre, E. J.; Wilcox, D.; Lin, X.; Hessler, P.; Torrent, M.; He, W.; Uziel, T.; Albert, D. H.; McDaniel, K.; Kati, W.; Shen, Y. Exploitation of castration-resistant prostate cancer transcription factor dependencies by the novel BET Inhibitor ABBV-075. *Mol. Cancer Res.* **2017**, *15*, 35-44.

(25) Zhang, P.; Wang, D.; Zhao, Y.; Ren, S.; Gao, K.; Ye, Z.; Wang, S.; Pan, C. W.; Zhu, Y.; Yan, Y.; Yang, Y.; Wu, D.; He, Y.; Zhang, J.; Lu, D.; Liu, X.; Yu, L.; Zhao, S.; Li, Y.; Lin, D.; Wang, Y.; Wang, L.; Chen, Y.; Sun, Y.; Wang, C.; Huang, H. Intrinsic BET inhibitor resistance in SPOP-mutated prostate cancer is mediated by BET protein stabilization and AKT-mTORC1 activation. *Nat. Med.* **2017**, *23*, 1055-1062.

(26) Raina, K.; Lu, J.; Qian, Y. M.; Altieri, M.; Gordon, D.; Rossi, A. M.; Wang, J.; Chen, X.; Dong, H. Q.; Siu, K.; Winkler, J. D.; Crew, A. P.; Crews, C. M.; Coleman, K. G. PROTAC-induced BET protein degradation as a therapy for castration-resistant prostate cancer. *Proc. Natl. Acad. Sci. U. S. A.* **2016**, *113*, 7124-7129.

(27) A Study of ZEN003694 in Patients with Metastatic Castration-Resistant Prostate Cancer. Clinical Trials, Mar 10, 2016; https://clinicaltrials.gov/ct2/show/NCT02705469, Accessed On Mar 11, 2018.

(28) A Dose-Finding Study of OTX105/MK-8628, A Small Molecule Inhibitor of the Bromodomain and Extra-Terminal (BET) Proteins, in Adults with Selected Advanced Solid Tumors (MK-8628-003). Clinical Trials, Oct 8, 2014; https://clinicaltrials.gov/ct2/show/NCT02259114, Accessed On Mar 11, 2018.

(29) Safety, Tolerability, Pharmacokinetics, and Pharmacodynamics of GS-5829 as A Single Agent and in Combination with Enzalutamide in Participants with Metastatic Castrate-Resistant Prostate Cancer. Clinical Trials, Nov 17, 2015; https://clinicaltrials.gov/ct2/show/NCT02607228,

Accessed On Mar 11, 2018.

(30) A Study to Investigate the Safety, Pharmacokinetics, Pharmacodynamics, and Clinical Activity of GSK525762 in Subjects with NUT Midline Carcinoma (NMC) and Other Cancers. Clinical Trials, Apr 30, 2012; https://clinicaltrials.gov/ct2/show/NCT01587703, Accessed On Mar 11, 2018.

(31) Xu, Y.; Zhang, M.; Xue, X.; Zhang, Y.; Liu, Z. Preparation of Benzo[d]isoxazole Compounds as Inhibitors of BET. Patent CN 105085427, Nov 25, 2015.

(32) Engelhardt, H. Benzimidazole Derivatives. Patent WO 2015169962, Nov 12, 2015.

(33) Engelhardt, H.; Martin, L.; Smethurst, C. Pyridinones. Patent WO 2015022332, Feb 19, 2015.

(34) Engelhardt, H. Triazolopyrazine Derivatives as BRD4 Inhibitors. Patent WO 2015067770, May 14, 2015.

(35) Brown, J. A.; Humphreys, P. G.; Jones, K. L.; Wellaway, C. R. Pyridinone Compound, Pharmaceutical Composition Containing the Same and Use. Patent WO 2016139292, Sep 9, 2016.

(36) Filippakopoulos, P.; Picaud, S.; Mangos, M.; Keates, T.; Lambert, J.-P.; Barsyte-Lovejoy, D.; Felletar, I.; Volkmer, R.; Müller, S.; Pawson, T.; Gingras, A.-C.; Arrowsmith, C. H.; Knapp, S. Histone recognition and large-scale structural analysis of the human bromodomain family. *Cell* **2012**, *149*, 214-231.

(37) Mertz, J. A.; Conery, A. R.; Bryant, B. M.; Sandy, P.; Balasubramanian, S.; Mele, D. A.; Bergeron, L.; Sims, R. J. Targeting MYC dependence in cancer by inhibiting BET bromodomains. *Proc. Natl. Acad. Sci. U. S. A.* **2011**, *108*, 16669-16674.

(38) Zhao, L.; Wang, Y.; Cao, D.; Chen, T.; Wang, Q.; Li, Y.; Xu, Y.; Zhang, N.; Wang, X.;

Chen, D.; Chen, L.; Chen, Y. L.; Xia, G.; Shi, Z.; Liu, Y. C.; Lin, Y.; Miao, Z.; Shen, J.; Xiong, B. Fragment-based drug discovery of 2-thiazolidinones as BRD4 inhibitors: 2. Structure-based optimization. *J. Med. Chem.* **2015**, *58*, 1281-1297.

(39) Delmore, J. E.; Issa, G. C.; Lemieux, M. E.; Rahl, P. B.; Shi, J. W.; Jacobs, H. M.; Kastritis, E.; Gilpatrick, T.; Paranal, R. M.; Qi, J.; Chesi, M.; Schinzel, A. C.; McKeown, M. R.; Heffernan, T. P.; Vakoc, C. R.; Bergsagel, P. L.; Ghobrial, I. M.; Richardson, P. G.; Young, R. A.; Hahn, W. C.; Anderson, K. C.; Kung, A. L.; Bradner, J. E.; Mitsiades, C. S. BET bromodomain inhibition as a therapeutic strategy to target c-Myc. *Cell* **2011**, *146*, 903-916.

(40) Fernandez-Salas, E.; Wang, S.; Chinnaiyan, A. M. Role of BET proteins in castration-resistant prostate cancer. *Drug Discov. Today: Technol.* **2016**, *19*, 29-38.

(41) Leslie, A. G.; Powell, H. R. Processing diffraction data with MOSFLM. *Evolv. Methods Macromol. Crystallogr.* **2007**, *245*, 41-51.

(42) Bailey, S. The CCP4 suite: programs for protein crystallography. *Acta Crystallogr. Sect. D: Biol. Crystallogr.* **1994**, *50*, 760-763.

(43) Mccoy, A. J.; Grosse-Kunstleve, R. W.; Adams, P. D.; Winn, M. D.; Storoni, L. C.; Read, R. J. Phaser crystallographic software. *J. Appl. Crystallogr.* **2007**, *40*, 658-674.

(44) Murshudov, G. N.; Skubak, P.; Lebedev, A. A.; Pannu, N. S.; Steiner, R. A.; Nicholls, R. A.; Winn, M. D.; Long, F.; Vagin, A. A. REFMAC5 for the refinement of macromolecular crystal structures. *Acta Crystallogr. Sect. D: Biol. Crystallogr.* **2011**, *67*, 355-367.

(45) Emsley, P.; Cowtan, K. Coot: model-building tools for molecular graphics. *Acta Crystallogr. Sect. D: Biol. Crystallogr.* **2004**, *60*, 2126-2132.

(46) Chen, V. B.; Arendall, W. B.; Headd, J. J.; Keedy, D. A.; Immormino, R. M.; Kapral, G. J.; Murray, L. W.; Richardson, J. S.; Richardson, D. C. MolProbity: all-atom structure validation for

macromolecular crystallography. *Acta Crystallogr. Sect. D: Biol. Crystallogr.* **2010**, *66*, 12-21.

Table of Contents graphic